Bioorganic Chemistry 93 (2019) 103373

Contents lists available at ScienceDirect

Bioorganic Chemistry

journal homepage: www.elsevier.com/locate/bioorg

Novel 2-arylbenzothiazole DNA gyrase inhibitors: Synthesis, antimicrobial evaluation, QSAR and molecular docking studies

Iman A.Y. Ghannam[a,*], Eman A. Abd El-Meguid[a], Islam H. Ali[a], Donia H. Sheir[a], Ahmed M. El Kerdawy[b,c,d]

[a] Chemistry of Natural and Microbial Products Department, Pharmaceutical and Drug Industries Research Division, National Research Centre, Dokki, Cairo 12622, Egypt
[b] Department of Pharmaceutical Chemistry, Faculty of Pharmacy, Cairo University, Kasr El-Aini Street, P.O. Box 11562, Cairo, Egypt
[c] Molecular Modeling Unit, Faculty of Pharmacy, Cairo University, Kasr El-Aini Street, P.O. Box 11562, Cairo, Egypt
[d] Department of Pharmaceutical Chemistry, Faculty of Pharmacy, New Giza University, Newgiza, km 22 Cairo-Alexandria Desert Road, Cairo, Egypt

ARTICLE INFO

Keywords:
2-Arylbenzothiazoles
Antimicrobial agents
DNA gyrase inhibitors
QSAR
Molecular docking

ABSTRACT

A series of new 2-arylbenzothiazole derivatives (**4**, **5**, **6a-j**, **7a-i** and **8a**,**b**) was synthesized and tested for their antimicrobial activity against different Gram-positive, Gram-negative bacteria and yeast using ciprofloxacin and fluconazole as positive controls for the antibacterial and antifungal activities, respectively. The target compounds showed stronger inhibitory activity against Gram-negative than Gram-positive bacteria. The minimum inhibitory concentration (MIC) values were determined for those compounds showed zone of inhibition ≥ 13 mm. Based on the MIC values for the tested compounds against *E. coli*, compounds (**4**, **5**, **6c**, **6d**, **6g**, **6i**, **6j**, **7b**, **7c**, **7g** and **8a**) were selected and tested for their *E. coli* gyrase inhibitory activity. The tested compounds showed moderate inhibitory activity against *E. coli* gyrase. Compounds **5**, **6c**, **6i**, **6j** and **7b** displayed high inhibitory activity against *E. coli* gyrase with IC_{50} values below 10 μM, however, they were less active than ciprofloxacin (*E. coli* gyrase IC_{50} = 1.14 μM). The *p*-hydroxy-*m*-methoxy benzothiazole analogue **6c** was the most active tested compound (*E. coli* gyrase IC_{50} = 4.85 μM). Quantitative structure–activity relationship (QSAR) study was also implemented for the newly synthesized compounds. The QSAR study indicated that the structural feature that governs the anti-microbial activity for the newly synthesized benzothiazole derivatives is their structural hydrophilic-lipophilic balance what agrees with the chemical intuition where this balance governs their cellular absorption and so their antimicrobial activity. Molecular docking showed that the newly synthesized compounds possess the required structural feature for *E. coli* gyrase B inhibition through interaction with the key amino acids Asp73 and Gly77.

1. Introduction

The increasing prevalence of bacterial resistance to therapeutic antibiotics is considered a challenge for the development of novel drugs for the treatment of infectious diseases. The major concern is the emergence of life-threatening infections caused by resistant Gram-positive and Gram-negative bacteria such as; *Staphylococcus aureus, Enterococcus faecium, Klebsiella pneumoniae* and *Pseudomonas aeruginosa* resulting in increased rate of mortality [1–3].

Bacterial type II topoisomerases constitute two ATP-fueled topoisomerase enzymes, DNA gyrase and topoisomerase IV that catalyze the changes of DNA by breaking and rejoining of DNA double strands [4]. DNA gyrase catalyzes negative supercoiling of cellular DNA during replication, while topoisomerase IV is required for dictation during DNA replication. The vital role of both enzymes is in controlling the topology of DNA during replication and therefore maintaining the bacteria growth and proliferation [5–8]. DNA gyrase is constituted of an ATP-activated heterotetramer composed of two A subunits (GyrA) and two B subunits (GyrB), which form the functional A2B2 tetramer structure [9]. Gyrase A subunits are involved in DNA strands cleavage, while the gyrase B subunits contain two ATP-binding domains, one each, to provide the energy required for the catalytic function of the gyrase through ATP hydrolysis [10–12]. On the other hand, topoisomerase IV is composed of two C subunits (ParC) and two E subunits (ParE), which are similar in structure and function to subunits (GyrA) and subunits (GyrB), respectively [4].

* Corresponding author at: Chemistry of Natural and Microbial Products Department, Pharmaceutical and Drug Industries Research Division, National Research Centre, Dokki, Cairo 12622, Egypt.
E-mail address: iman.youssef.ghannam@gmail.com (I.A.Y. Ghannam).

https://doi.org/10.1016/j.bioorg.2019.103373
Received 22 August 2019; Received in revised form 6 October 2019; Accepted 16 October 2019
Available online 24 October 2019
0045-2068/

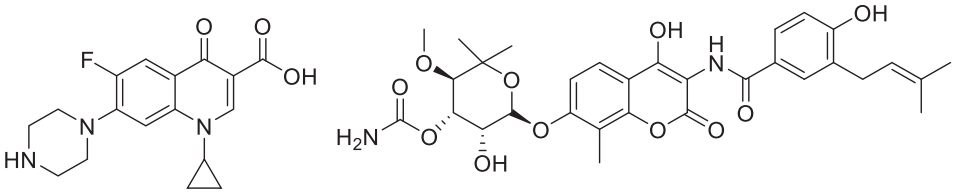

Fig. 1. DNA gyrase inhibitors; ciprofloxacin (**I**) and novobiocin (**II**).

Ciprofloxacin (**I**), a fluoroquinolone antibacterial agent, acts by targeting DNA gyrase and topoisomerase IV [13]. Generally, fluoroquinolones exert their antibacterial activity through targeting primarily DNA gyrase and secondly topoisomerase IV to different extents, which explain some of the differences in the spectrum of activity of the fluoroquinolones [14,15]. Therefore, DNA gyrase is likely to be more important to Gram-negative bacteria, while topoisomerase IV is likely to be more important to Gram-positive bacteria. It was found that the affinity of the compounds towards DNA gyrase does not always correlate with the antibacterial activity against all tested bacterial strains [16].

Drugs targeting DNA gyrase act by either of two main mechanisms; (a) by fixation of the complex between the DNA and the GyrA active site of the enzyme e.g. ciprofloxacin (**I**) (b) by inhibiting the ATPase function of GyrB subunit e.g. novobiocin (**II**), a natural aminocoumarin isolated from *Streptomyces* species. Novobiocin is the only representative of ATP-competitive DNA GyrB inhibitors approved for clinical use, although, it has been withdrawn for safety concerns, poor water solubility and low effectiveness (Fig. 1) [17–20].

The aforementioned facts make the search for new gyrase inhibitors with optimum inhibitory activity and fewer side effects a hot research topic to fight the emerging bacterial resistance [11,21]. Benzothiazole scaffold has been used to design novel DNA Gyrase B inhibitors e.g. the benzothiazole-2-pyrrolamide derivative (**III**) and the benzothiazole-2-ethyl urea derivative (**IV**) showed potent and intermediate *E. coli* gyrase inhibitory activities with IC_{50} of 0.058 and 3.9 μM, respectively. However, both of the benzothiazole derivatives (**III** and **IV**) showed weak antibacterial activity against Gram-positive bacteria [4,22]. These GyrB inhibitors binds to the ATP binding site through hydrogen bond interactions of the pyrrole NH group in the benzothiazole derivative (**III**) or the two NH groups of the ethyl urea moiety in the benzothiazole analogue (**IV**) with the side chain carboxylate of Asp73 at the ATP binding site [4,23]. This hydrogen bonding interaction pattern resembles the binding of the carbamate moiety of novobiocin in the DNA gyrase binding pocket blocking the interaction of adenine ring of ATP and DNA gyrase binding pocket. The ethylurea-based gyrase B inhibitor (**IV**) possessed additional cation-π interactions between the phenyl ring and the Arg76 side chain [24,25].

Novel benzothiazole schiff's base (**V**) has been designed as antibacterial agent against Gram-positive and Gram-negative bacteria and showed good antibacterial activity against Gram-positive and Gram-negative bacteria; *S. aureus, E. fecalis, E. coli* and *K. pneumoniae* with MIC of 7.81, 31.2, 15.6, 15.6 μg/mL, respectively. Moreover, the 2-(4-amidophenyl)benzothiazole derivative (**VI**) has been reported for its broad spectrum antibacterial activity against *S. aureus, E. fecalis, E. coli* and *K. pneumoniae* with MIC of 15.6, 31.2, 7.8, 3.9 μg/mL, respectively (Fig. 2) [26,27].

Motivated by the DNA gyrase inhibitory and antibacterial activities of the benzothiazole derivatives **IV**-**V**, it seemed of interest to design novel 2-arylbenzothiazole derivatives **6–8** bearing the NH of the amide moiety for hydrogen bonding with Asp73. Additional hydrogen bond acceptors/donors; amido (C═O), iminio (C═N), (−O-CH_3) groups and the ether linkage were introduced to interact with the amino acids; Asp73 and/or Gly77 to improve binding affinity of the designed compounds. The 2-phenylbenzothiazole core is designed for the cation-π interaction with the positively charged amino acids Arg76 and Arg136 at the ATP binding site of Gyrase B (Fig. 3).

Herein, we report the synthesis and the antimicrobial activity of the newly synthesized benzothiazole compounds (**4**, **5**, **6a-j**, **7a-i** and **8a**,**b**). Based on the MIC values of the synthesized compounds, potent compounds were selected for DNA gyrase inhibitory activity evaluation. A quantitative structure–activity relationship (QSAR) study was also carried out to investigate the structural features responsible for the antimicrobial activity of the newly synthesized compounds. Molecular docking study was carried out to study the binding pattern of the newly synthesized compounds in the active site of *E. coli* gyrase B to rationalize their activity on the enzyme and to investigate their ability to satisfy its required binding features.

2. Results and discussion

2.1. Chemistry

In Scheme 1, the target 2-phenylbenzothiazole compounds (**4**, **5**, **6a-j**, **7a-i** and **8a**,**b**) were synthesized. The parent benzothiazole compound **3** was synthesized as reported method via reflux of *o*-aminothiophenol **1** and 4-hydroxy-3-methoxybenzaldehyde **2** in dimethylformamide (DMF) [28].

The different substituents (R_1, R_2) used for the synthesis of the 2-arylbenzothizole derivatives (**6a-j**, **7a-i**, **8a**,**b**) and each yield % were mentioned in details in (Table 1).

The benzothiazole derivative **3** was allowed to react with ethyl 2-bromopropionate by refluxing in dimethylformamide in the presence of anhydrous potassium carbonate to give ethyl 2-(4-(benzo[*d*]thiazol-2-yl)-2-methoxy phenoxy) propanoate **4**.

Upon refluxing the benzothiazole ester derivative **4** with hydrazine hydrate in absolute ethanol, the propane hydrazide compound **5** was produced.

Condensation of the hydrazide analogue **5** with different aldehydes, acyclic and cyclic ketones was done through refluxing with the appropriate aldehyde or ketone derivatives in absolute ethanol in the presence of few drops of acetic acid to give the corresponding new schiff's bases; **6a-j**, **7a-i** and **8a**,**b**, respectively. It was observed that all the signals in ^{1}H- and ^{13}C NMR spectra of schiff's bases **6–7** were repeated due to presence of the synthesized schiff' bases as *E,Z* stereoisomers. For *N*′-benzylidenepropane hydrazides **6a-j**, produced from the reaction of the propane hydrazide **5** with different aldehydes, there were two new singlet signals at δ 7.92–8.65 and 8.10–8.81 ppm attributed to azomethine protons (C<u>H</u>═N) in *E* and *Z* isomers. In *N*′-(1-phenylethylidine)propane hydrazides **7a-i**, resulting from the reaction of the propane hydrazide **5** with acyclic ketones, ^{1}H NMR spectra showed two extra singlet signals at δ 2.29–2.33 and 2.31–2.39 ppm corresponding to the C<u>H</u>$_3$ protons in *E* and *Z* isomers whereas, their ^{13}C NMR spectra illustrated two signals at δ 13.63–14.37 and 13.92–14.87 ppm due to the CH_3 carbons introduced as a result of reaction with the acyclic ketones.

2.2. Biological evaluation

2.2.1. Antimicrobial activity

All target compounds (**4**, **5**, **6a-j**, **7a-i** and **8a**,**b**) were tested for their antimicrobial activity against three Gram-positive bacteria (two *S.*

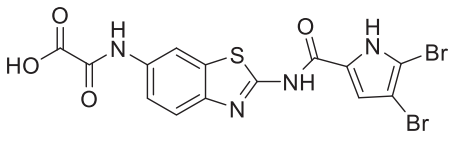

(III)

E. coli DNA gyrase IC_{50} = 0.058 µM

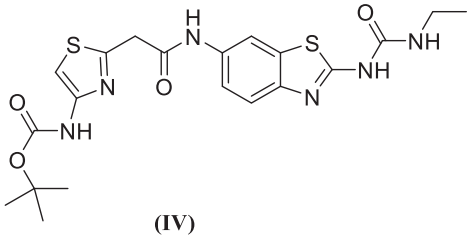

(IV)

E. coli DNA gyrase IC_{50} = 3.9 µM

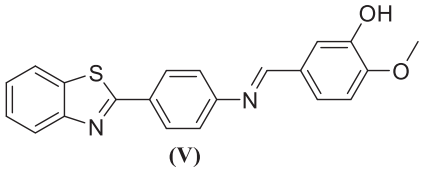

(V)

S. aureus MIC = 7.81 µg/mL
E. fecalis MIC = 31.2 µg/mL
E. coli MIC = 15.6 µg/mL
K. pneumoniae MIC = 15.6 µg/mL

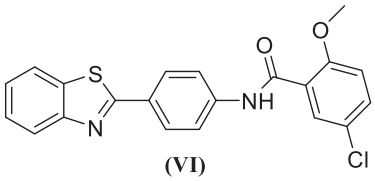

(VI)

S. aureus MIC = 15.6 µg/mL
E. fecalis MIC = 31.2 µg/mL
E. coli MIC = 7.8 µg/mL
K. pneumoniae MIC = 3.9 µg/mL

Fig. 2. Chemical structures of benzothiazoles as DNA gyrase inhibitors and antibacterial agents (**III-VI**).

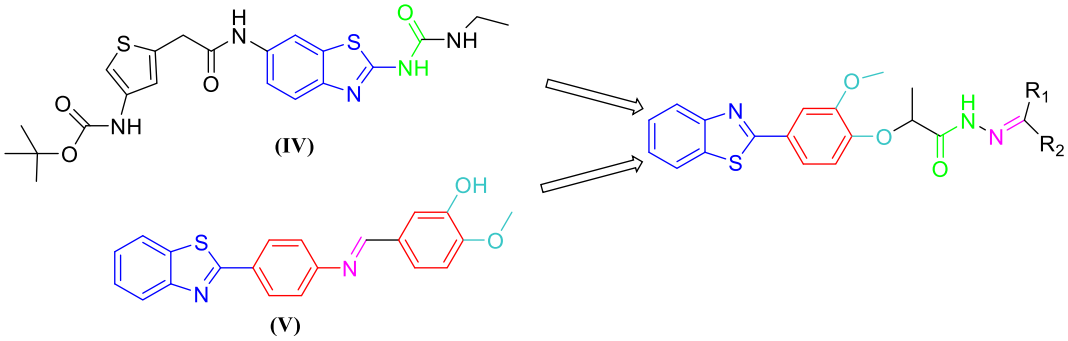

Fig. 3. Design strategy of the target compounds **6–8.**

aureus strains (ATCC-29213 and ATCC-6538) and *E. fecalis* ATCC-29212), six Gram-negative bacteria (*E. coli* ATCC-25923, *P. microbilis* ATCC 9240, *P. aeuroginosa* ATCC-27953, two strains *K. pneumoniae* (ATCC-10031 and ATCC-13883) and *S. flexneri* ATCC12022) and yeast (*C. albicans* ATCC-10231). Ciprofloxacin and fluconazole were used as positive controls for antibacterial and antifungal activities, respectively. Results are displayed in Table S.2.1. (Supporting information) as zones of inhibition in mm.

Overall, the newly synthesized compounds showed higher inhibitory activity against Gram-negative bacteria than against Gram-positive bacteria. All the 23 synthesized compounds exhibited good antibacterial activity against Gram-negative bacteria. Eleven compounds (**4**, **5**, **6c**, **6d**, **6g**, **6i**, **6j**, **7b**, **7c**, **7g** and **8a**) displayed more than 90% growth inhibition against *E. coli*. Ten compounds (**4**, **5**, **6a**, **6b**, **6c**, **6d**, **6f**, **6h**, **6i** and **7c**) displayed more than 90% growth inhibition against *P. mirabilis* and *P. aueroginosa*. Eighteen compounds (**4**, **5**, **6c**, **6d**, **6e**, **6i**, **6j**, **7a**, **7b**, **7c**, **7d**, **7e**, **7f**, **7g**, **7h**, **7i**, **8a** and **8b**) showed more than 90% growth inhibition against *K. pneumoniae*. Only three compounds **(4, 5** and **6i**) showed more than 90% growth inhibition against *S. flexneri*. Ten compounds (**4**, **5**, **6c**, **6d**, **6i**, **6j**, **7b**, **7c**, **7h** and **8a**) displayed more than 90% growth inhibition against *S. aureus*. Thirteen compounds (**4**, **5**, **6c**, **6d**, **6e**, **6g**, **6i**, **6j**, **7b**, **7c**, **7d**, **7e** and **8a**) showed ≥ 90% growth inhibition against *E. feacalis*. Eleven compounds (**4**, **5**, **6b**, **6c**, **6d**, **6h**, **6i**, **6j**, **7c**, **7i** and **8a**) showed moderate to high inhibitory activity against *C. albicans*.

MIC values were determined for the tested compounds that showed zone of inhibition ≥ 13 mm (Table 2). *K. pneumoniae* (ATCC-10031) was one of the highly sensitive Gram-negative bacterial strains to the tested compounds. The ester derivative **4** was the least antibacterial compound (*K. pneumoniae* MIC = 5.93 µM), while the propane hydrazide derivative **5** was of higher antibacterial activity and equipotent to ciprofloxacin (*K. pneumoniae* MIC = 2.83 and 2.93 µM, respectively). The unsubstituted **6a**, *p*-hydroxy **6b**, *p*-nitro **6f**, *p*-cyano **6g** and 2-thienyl-1*H*-indolyl **6h** analogues of the *N′*-benzylidenepropane hydrazide series showed no significant antibacterial activity against *K. pneumoniae*. The 4-hydroxy-3-methoxy **6c** and 4-nitro-3-chloro **6e** derivatives showed higher antibacterial activity than ciprofloxacin (*K. pneumoniae* MIC = 2.03 and 1.94 µM, respectively). The antibacterial activity was increased two-fold for the *p*-fluoro derivative **6d** (*K. pneumoniae* MIC = 1.09 µM). The 5-membered heterocycle analogues, 5-methylfuryl **6i** and pyrazolone **6j** analogue were the most active compounds against *K. pneumoniae* in a sub-micromolar MIC of 0.56 and 0.44 µM, respectively and were five to six folds more active than ciprofloxacin. The *N′*-(1-phenylethylidine)propane hydrazide series; *p*-hydroxy **7b**, *m*-hydroxy **7c** derivatives were the most active antibacterial compounds (*K. pneumoniae* MIC = 1.04 µM). The unsubstituted **7a**, *p*-bromo **7f**, *p*-nitro **7g**, 2-thienyl **7h**, 2-furyl **7i** and 2-oxidoline **8a** analogues were almost equipotent against *K. pneumoniae* (MIC = 2.18, 2.45, 1.98, 2.15, 2.23 and 2.06, respectively). The least active antibacterial compounds were the *p*-methoxy **7d** and *p*-chloro **7e** derivatives (*K. pneumoniae* MIC = 4.11 and 4.07 µM, respectively).

The propane hydrazide analogue **5** and the pyrazolone analogue **6j**

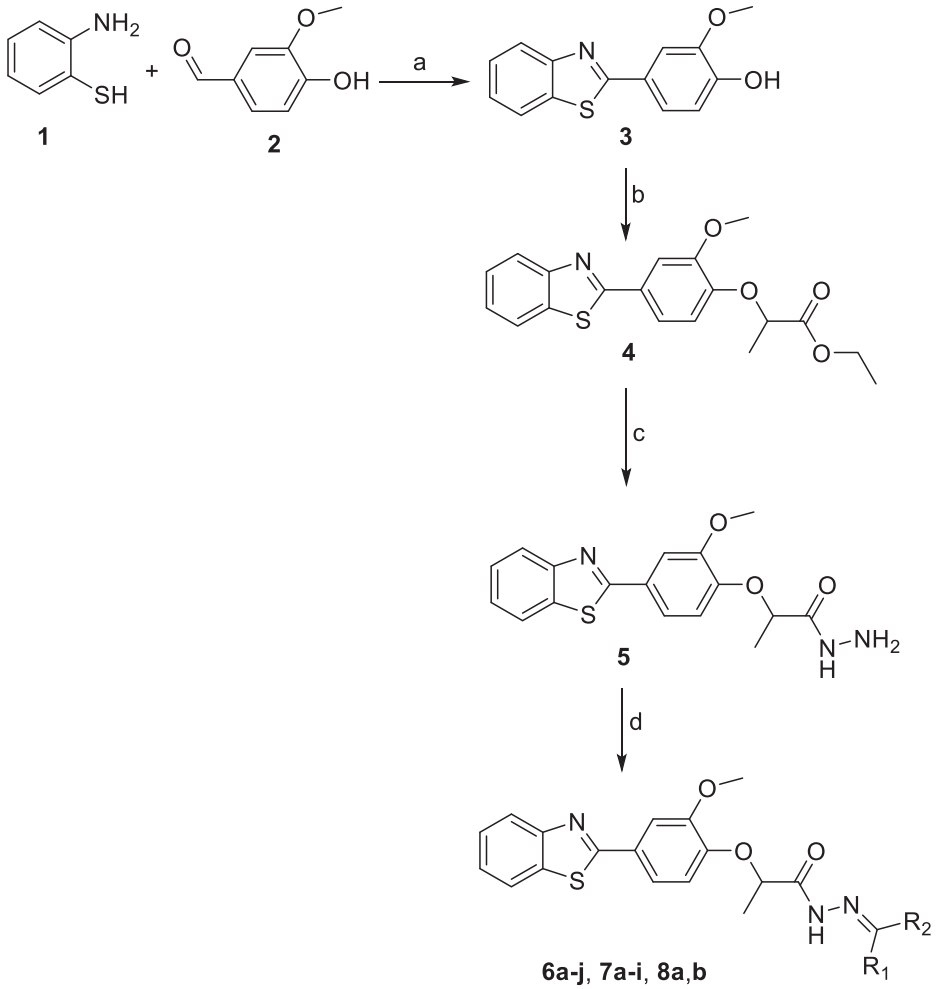

Scheme 1. Reactions and conditions. Scheme 1: Synthesis of benzothiazole derivatives (**4**, **5**, **6a-j**, **7a-i**, **8a**,**b**); a: DMF, reflux, 3 h, 76%; b: DMF, K_2CO_3 anhydrous, ethyl 2-bromopropionate, 1 h, 60%; c: absolute ethanol, hydrazine hydrate, reflux, 4 h, 69%; d: absolute ethanol, glacial acetic acid, substituted aldehydes, acyclic or cyclic ketones, reflux, 1–3 h, 54–91%.

were the most active compounds against *E. coli* with MIC value 0.69 and 1.79 μM, respectively, which are more active than ciprofloxacin (*E. coli* MIC = 2.93 μM). The *p*-fluoro derivative **6d** and the 5-methylfuryl derivative **6i** were the most active compounds against *P. mirabilis* with MIC values 2.16 and 2.23 μM, respectively, which are around twenty times more active than ciprofloxacin (*P. mirabilis* MIC = 47.13 μM). The 4-hydroxy-3-methoxy analogue **6c** and the 2-thienyl-1*H*-indolyl analogue **6h** were the most active compounds against *P. aeruginosa* with MIC values of 1.02 and 0.88 μM, respectively, which are almost three times more active than ciprofloxacin (*P. aeruginosa* MIC = 2.93 μM). *S. flexneri* was the most resistant bacteria and compound **6i** was the most active compound against *S. flexneri* with MIC value of 2.23 μM which is more than two folds active as ciprofloxacin (*S. flexneri* MIC = 5.89 μM).

E. faecalis was one of the highly sensitive Gram-positive bacteria for the tested compounds. The ester derivative **4** and the propane hydrazide **5** showed equipotent antibacterial activity against *E. faecalis* with MIC of 1.34 and 1.39 μM, respectively, and of higher activity than ciprofloxacin (*E. faecalis* MIC = 2.93 μM). The unsubstitued **6a**, *p*-hydroxy **6b**, *p*-nitro **6f** and 2-thienyl-1*H*-indolyl **6h** analogues of the *N*′-benzylidenepropane hydrazide series showed no significant antibacterial activity against *E. faecalis*. The 4-hydroxy-3-methoxy **6c** and *p*-cyano **6g** derivatives exhibited equipotent activity which is the highest among the tested compounds against *E. faecalis* with MIC values of 1.02 and 1.07 μM, respectively, which is almost three-fold lower than that of ciprofloxacin. The antibacterial activity for the 5-methylfuryl analogue **6i** against *E. faecalis* was decreased half fold than that of derivatives **6c** and **6g** (*E. faecalis* MIC = 2.23 μM). The *p*-fluoro **6d** and 4-nitro-3-chloro **6e** analogues were the least active compounds against *E. faecalis* with MIC values of 4.34 and 7.65 μM, respectively. In the *N*′-(1-phenylethylidine)propane hydrazide series, the *p*-hydroxy **7b**, *m*-hydroxy **7c**, *p*-chloro **7e** derivatives were the most active antibacterial compounds with MIC *E. faecalis* of 1.04, 1.04 and 1.00 μM, respectively. The unsubstituted **7a**, *p*-bromo **7f**, *p*-nitro **7g**, 2-thienyl **7h**, 2-furyl **7i** and 5-nitro-2-oxidoline **8b** analogues showed no antibacterial activity against *E. faecalis*. The *p*-methoxy **7d** derivative showed moderate activity (*E. faecalis* MIC = 2.04 μM). The 2-oxindoline analogue **8a** showed the least antibacterial activity (*E. faecalis* MIC value 4.13 μM).

Compounds **6c**, **6j**, **7b**, **7c**, **7h** and **8a** were the most active compounds against *S. aureus* with MIC values; 2.03, 1.79, 2.10, 2.10, 2.15 and 2.06 μM, respectively. These compounds were almost three times more active than ciprofloxacin (*S. aureus* MIC = 5.89 μM).

For the antifungal activity, compound **6i** was the most active compound against *C. albicans* with MIC of 0.56 μM which is almost three times more active than fluconazole (*C. albicans* MIC = 1.56 μM). However, the ethyl propionate analogue **4** and the propane hydrazide analogue **5** were the least active compounds against *C. albicans* with MIC values of 10.92 and 11.37 μM, respectively. For the effect of the substituents on the terminal phenyl moiety on the antimicrobial activity, it was found that the antibacterial activity of the unsubstituted derivatives **6a** and **7a** was only detected against few strains of Gram-negative bacteria (MIC ranging from 2.18 to 9.05 μM) with no significant antifungal activity. The introduction of electron donating

Table 1
Structure of different substituents (R_1, R_2) used for synthesis of benzothiazole derivatives **6–8** and yield %.

Cpd No.	R_1	R_2	Yield %	Cpd No.	R_1	R_2	Yield %
6a	H		83	**7b**	CH_3	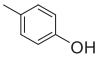	83
6b	H	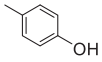	77	**7c**	CH_3		91
6c	H	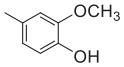	90	**7d**	CH_3	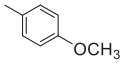	90
6d	H		54	**7e**	CH_3		84
6e	H	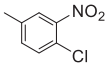	91	**7f**	CH_3		78
6f	H	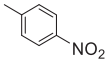	79	**7 g**	CH_3	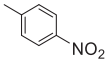	76
6 g	H	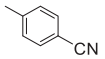	90	**7 h**	CH_3		73
6 h	H	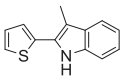	90	**7i**	CH_3		82
6i	H	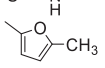	88	**8a**	–	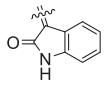	78
6j	H	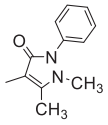	78	**8b**	–	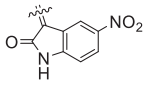	73
7a	CH_3		85				

Table 2
MIC values of the target compounds against Gram +ve, Gram −ve bacteria and yeast.

Compound No.	Gram-positive Bacteria			Gram-negative Bacteria					Yeast
	S. aureus (ATCC-29213)[a]	*S. aureus* (ATCC-6538)	*E. faecalis* (ATCC-29212)	*E. coli* (ATCC-25923)	*P. mirabilis* (ATCC 9240)	*P. aeruginosa* (ATCC-27953)	*K. pneumonia* (ATCC-10031)	*K. pneumonia* (ATCC-13883)	*C. albicans* (ATCC-10231)
					MIC (μM)[b]				
4	5.46	5.46	1.34	2.72	5.46	2.72	5.46	2.72	10.92
5	-[c]	2.83	1.39	0.69	5.69	2.83	2.83	2.83	11.37
6a	–	–	–	–	9.05	4.52	–	–	–
6b	–	–	–	–	15.62	1.95	–	–	4.72
6c	2.03	4.09	1.02	2.03	8.18	1.02	2.03	2.03	2.03
6d	–	4.34	4.34	2.16	2.16	1.09	1.09	8.69	2.16
6e	–	–	7.65	–	–	–	1.94	1.94	–
6f	–	–	–	–	32.82	8.19	–	–	–
6g	–	–	1.07	2.13	–	–	–	–	–
6h	–	–	–	–	3.53	0.88	–	–	1.76
6i	–	4.48	2.23	2.23	2.23	2.23	0.56	2.23	0.56
6j	1.79	3.60	1.84	1.79	–	–	0.44	1.79	3.60
7a	–	–	–	–	–	–	2.18	2.18	–
7b	2.10	–	1.04	2.10	–	–	1.04	–	–
7c	2.10	–	1.04	2.10	4.23	2.10	1.04	2.10	2.10
7d	–	–	2.04	–	–	–	4.11	4.11	–
7e	–	–	1.00	–	–	–	4.07	2.03	–
7f	–	–	–	–	–	–	2.45	–	–
7g	–	–	–	3.98	–	–	1.98	–	–
7h	–	2.15	–	–	–	–	2.15	2.15	–
7i	–	–	–	–	–	–	2.23	4.48	4.48
8a	2.06	4.13	4.13	8.26	–	–	2.06	2.06	8.26
8b	–	–	–	–	–	–	–	1.88	–
Ciprofloxacin	5.89	5.89	2.93	2.93	47.13	2.93	2.93	2.93	–
Fluconazole	–	–	–	–	–	–	–	–	1.57

[a] ATCC: American Tissue Culture Collection.
[b] MIC: Minimum inhibitory concentration that inhibits the growth of bacteria or yeast by ≥ 90%.
[c] –: Not determined.

substituents to the phenyl ring as in 4-hydroxy-3-methoxy substituted **6c** and the 4-methoxy substituted **7c** derivatives, enhanced the antimicrobial activity significantly against most of the tested strains with MIC values ranging from 1.02 to 8.18 μM, while the antimicrobial profile of the compounds bearing electron withdrawing substituents (**6d-g** and **7e-g**) was decreased significantly against the tested microbial strains with MIC values of 1.07 to 32.82 μM. The replacement of the phenyl ring with hetero/heteroaryl moieties enhanced the antimicrobial potential against Gram-negative bacteria and fungi over Gram-positive bacteria for compounds **6h-j** (MIC: 0.44 to 3.53 μM), whereas the antimicrobial activity for the hetero/heteroaryl derivatives of the *N′*-propane hydrazides; **7h**, **7i** and **8b** was decreased significantly especially for Gram-positive bacteria (MIC: 2.06 to 4.48 μM) with the exception of the 2-oxindoline compound **8a** whose antimicrobial activity was enhanced against Gram-positive bacteria and fungi than Gram-negative bacteria (MIC: 2.06 to 8.26 μM).

2.2.2. DNA gyrase inhibitory activity

Eleven compounds (**4**, **5**, **6c**, **6d**, **6g**, **6i**, **6j**, **7b**, **7c**, **7g** and **8a**) were selected, based on their recorded MIC values against *E. coli*, to be tested for their anti-gyrase activity and were compared to ciprofloxacin as a reference standard (Table 3).

The selected tested compounds exhibited moderate inhibitory activity against *E. coli* gyrase in comparison to ciprofloxacin. They showed IC_{50} values ranging from 4.85 to 29.67 μM, whereas, ciprofloxacin showed *E. coli* gyrase IC_{50} of 1.14 μM. The ester derivative **4** showed low anti-gyrase activity IC_{50} = 15.86 μM, while the activity was improved approximately half fold for the propane hydrazide derivative **5** which showed IC_{50} value of 7.42 μM. Regarding the effect of the substituents on the terminal phenyl moiety on the gyrase inhibitory activity, the results showed that the 4-hydroxy-3-methoxy substituted analogue **6c** was the most active compound within the tested *N′*-benzylidenepropane hydrazide series, with IC_{50} of 4.85 μM. The introduction of electron withdrawing substituents to the phenyl ring as in the *p*-fluoro **6d** and *p*-cyano **6g** derivatives decreased the gyrase inhibitory activity significantly giving IC_{50} values 22.97 and 29.67 μM, respectively. Whereas, upon the phenyl ring replacement with a hetero or heteroaryl moiety as in the pyrazolone **6j**, the 5-methylfuryl **6i** and 2-oxindoline **8a** compounds, the anti-gyrase activity was slightly decreased with IC_{50} values of 6.81, 7.15 and 10.88 μM, respectively. The introduction of the adjacent methyl substituent to the phenyl ring in **series 7** decreased the gyrase inhibitory activity of the substituted *N′*-(1-phenylethylidine) propane hydrazides, *p*-hydroxy **7b**, *m*-hydroxy **7c** and *p*-nitro **7g** derivatives giving IC_{50} values of 8.36, 10.20 and 13.28 μM, respectively.

2.3. Quantitative structure–activity relationship (QSAR) study

The QSAR study was carried out to explore the structural features governing the antimicrobial activity of the target benzothiazole derivatives and the structural modifications which could be utilized to improve their anti-microbial activity [29,30].

Fifteen novel synthesized benzothiazole derivatives were selected based on their MIC against *K. pneumoniae* (ATCC-10031), the most sensitive microorganism (Gram-negative bacteria) to the synthesized tested compounds.

The 15 newly synthesized benzothiazole derivatives were split into a training set of 12 compounds and a test set of 3 compounds such that the test set maintains the activity value distribution of the original dataset. A set of 313 molecular mechanical descriptors available in MOE was computed for the training set.

The obtained "descriptors/anti-microbial activity (1/MIC)" matrix was then transferred to RapidMiner 7.1.000 Basic Edition for QSAR model construction [31–34]. First, descriptor filtration was performed by removing the low-variance descriptors which add no additional information to the model (redundant descriptors) leaving a set of 291 descriptors for model generation. Descriptor selection was then carried out using the conventional forward selection algorithm (FSA) available in RapidMiner [35] and multiple linear regression (MLR) was used as the machine learning algorithm for the construction of a linear correlation model which is characterized by simplicity, transparency and interpretability. Root mean square error of a leave-10%-out (L10%O) cross-validation ($RMSE_{CV}$) was used for model performance assessment.

Based on the FSA descriptor selection a two descriptors model was generated (Equation 1) with a significantly good performance as represented in its statistical evaluation parameters and its predictions (Tables 4 and 5) where its coefficient of determination R^2 for training set prediction and L10%O cross-validation are 0.810 and 0.753, respectively, and with RMSE of 0.272 and 0.310, respectively. The closeness between the cross-validation and training set prediction results indicates the robustness of the model and its lack of over fitting (over training).

Figs. 4 and 5 show the high agreement between the experimental and model predicted antimicrobial activity in training set prediction and in *L*10%O cross-validation.

$$\frac{1}{\text{MIC}} = 1.260 * (\text{vsurf\_Wp6}) - 37.061 * (\text{vsurf\_HL1}) + 3.071 \quad (1)$$

For further model validation, external validation was carried out to ensure that it predicts the data points and not just fits them, to this end, the model was used to predict the antimicrobial activity of the test set compounds. The model showed excellent test set prediction (Table 5) indicating the robustness and the predictive ability of the obtained QSAR model.

The two descriptors selected for the QSAR model are *vsurf_Wp6* and *vsurf_HL1*. *vsurf_Wp6* is directly proportional to the antimicrobial activity (with positive coefficient), whereas, *vsurf_HL1* is inversely proportional to the antimicrobial activity (with negative coefficient). Vsurf_* descriptors are 3D molecular descriptors similar to the VolSurf descriptors [36]. *vsurf_Wp6* describes the molecular polar volume, whereas, *vsurf_HL1* describes the molecular hydrophilic-lipophilic balance.

The QSAR study indicates that the structural feature that governs the antimicrobial activity for the newly synthesized benzothiazole derivatives is their structural hydrophilic-lipophilic balance what agrees with the chemical intuition where this balance governs their cellular absorption and so their antimicrobial activity.

2.4. Molecular docking study

Docking simulations were performed to study the binding pattern of the newly synthesized compounds in *E. coli* DNA gyrase B active site to

Table 3
IC_{50} values of some selected compounds against *E. coli* gyrase.

Cpd No.	IC_{50} (μM)	Cpd No.	IC_{50} (μM)
4	15.86 ± 0.75	**6j**	6.81 ± 0.28
5	7.42 ± 0.33	**7b**	8.36 ± 0.33
6c	4.85 ± 0.26	**7c**	10.20 ± 0.46
6d	22.97 ± 1.1	**7g**	13.29 ± 0.64
6g	29.67 ± 1.29	**8a**	10.88 ± 0.47
6i	7.15 ± 0.29	**Ciprofloxacin**	1.14 ± 0.24

Table 4
Statistical performance of the QSAR model in training set prediction and in leave-10%-out (L10%O) cross-validation.

	Training set prediction	L10%OCV prediction
R^2	0.810	0.753
RMSE	0.272	0.310

Table 5
Experimental and predicted (1/MIC) for the training set and test set compounds and the training set prediction in L10%O_{CV} and the calculated residual error in the different cases.

Cpd No.	Experimental 1/MIC	training set prediction	residual error[a]	L10%O_{CV} prediction	Residual error[a]
4	0.183	0.554	−0.371	0.642	−0.458
6c	0.493	0.517	−0.025	0.525	−0.032
6d	0.917	1.149	−0.231	1.186	−0.268
6e	0.526	0.769	−0.243	0.819	−0.293
6i	1.786	1.096	0.690	1.005	0.781
6j	2.273	2.251	0.022	2.190	0.082
7a	0.459	0.323	0.136	0.296	0.163
7b	0.962	1.078	−0.117	1.093	−0.131
7d	0.243	0.385	−0.142	0.413	−0.170
7e	0.246	0.179	0.066	0.159	0.087
7i	0.448	0.141	0.307	0.158	0.290
8a	0.485	0.578	−0.093	0.504	−0.018
Cpd No.	Experimental 1/MIC	test set prediction	Residual error[a]		
5	0.353	0.748	−0.395		
7c	0.962	0.834	0.128		
7h	0.465	0.353	0.112		

[a] Residual error is calculated as the difference between the experimental and the predicted 1/MIC.

predict their binding pattern and to investigate their ability to satisfy the required structural features for binding interactions.

The docking setup was first validated by performing self-docking of the co-crystalized thiazole inhibitor in the active site of *E. coli* DNA gyrase B (PDB ID: 4DUH) [37]. The self-docking validation reproduced the co-crystallized thiazole inhibitor's experimental binding mode indicating that the docking protocol used is suitable for the intended docking study. This is shown by the small RMSD between the experimental co-crystallized inhibitor pose and the docked pose of 0.432 Å; and by the capability of the docking pose to reproduce all the key interactions achieved by the co-crystallized ligands in the active site with Asp73, Arg76, Gly77 (water mediated interaction), Gly101, and Arg136 (Figs. 6 and 7).

Most of the newly synthesized compounds showed a common binding mode in the *E. coli* DNA gyrase B active site, the (un)substituted aryl moieties accommodate in the hydrophobic sub-pocket of the active site surrounded by the hydrophobic site chains of the amino acids Val43, Met95, Val120, Val123, Leu130, Leu132, and Val167. The rest of the compound is extended in the active site toward outward direction accomplishing hydrogen bonding interaction with the key amino acid Asp73 and water-mediated hydrogen bonding with Gly77. Most of the compounds achieve the hydrogen bonding with the key amino acids Asp73 and Gly77 by their amido group (Compounds **6a**, **6b**, **6d-g**, **6i**, **7a-c**, **7e**, **7g-i**). Few compounds achieve the hydrogen bonding with these key amino acids by their substituted aryl moiety (compounds **6c**, **6h**, **8a**,**b**). Moreover, the extending benzothiazole moiety achieving cation-π interaction with the positively charged guanido groups of Arg76 or Arg136. Only compound **6j** showed reversed binding pose with its benzothiazole moiety directed toward the hydrophobic region of the active site achieving hydrogen bonding interaction with the key amino acid Arg136 with its hydrazide moiety. Worth mentioning that most of series **6** compounds could achieve hydrogen bonding with both Asp73 and Gly77, whereas, series **7** compounds could interact with Asp73 only what could be attributed to their methyl group which hinders the proper orientation of the amido C═O functional group and so it cannot form the key water-mediated hydrogen bond interaction with Gly77 (Figs. 8 and 9) (see Supplementary information for further details).

Table 6 shows the predicted docking score of the newly synthesized compounds. It can be seen that the most potent gyrase inhibitor among the newly synthesized compounds **6c** with IC_{50} of 4.85 μM, is showing the second most negative energy score of −16.17 kcal/mol with higher predicted binding affinity than the co-crystalized ligand which showed a docking score of −14.46 kcal/mol. Compound **6c** achieved the key interactions with the amino acids Asp73 and Gly77.

In Summary, these results indicate that most of the newly synthesized compounds possess the required structural features for gyrase B inhibition. Generally, they interact by their terminal (un)substituted aryl moiety through hydrophobic interaction with the hydrophobic side chains of the amino acids Val43, Met95, Val120, Val123, Leu130, Leu132, and Val167 lining the hydrophobic sub-pocket. Through hydrogen bonding they interact by their amido group with the key amino acids Asp73 and gly77. By their benzothiazole moiety, they interact through cation-π interaction with the key amino acids Arg76 and/or Arg136.

Based on the biological evaluations and molecular docking study we can deduce the following features in the most active compound **6c**; the

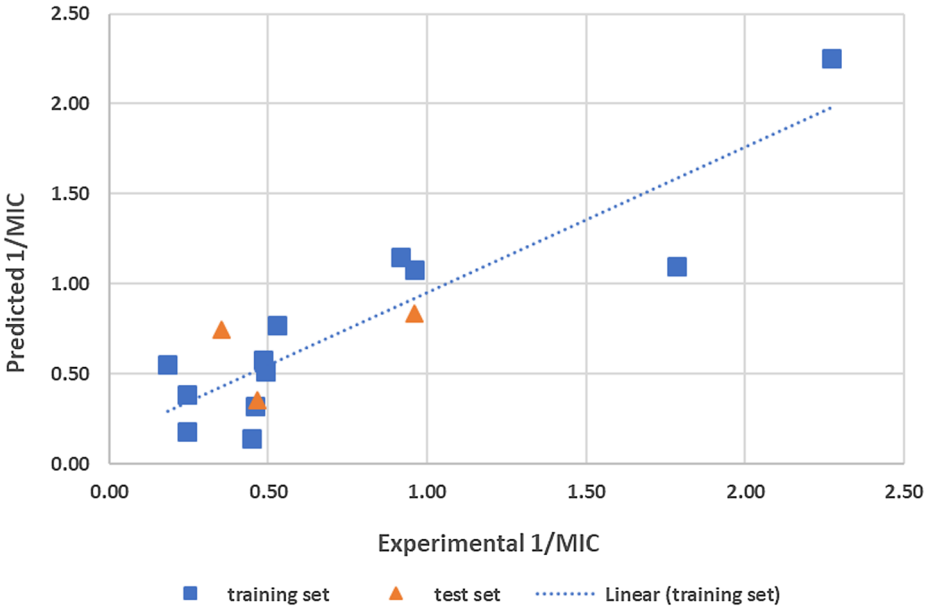

Fig. 4. Correlation plot for training set and test set experimental vs. predicted 1/MIC.

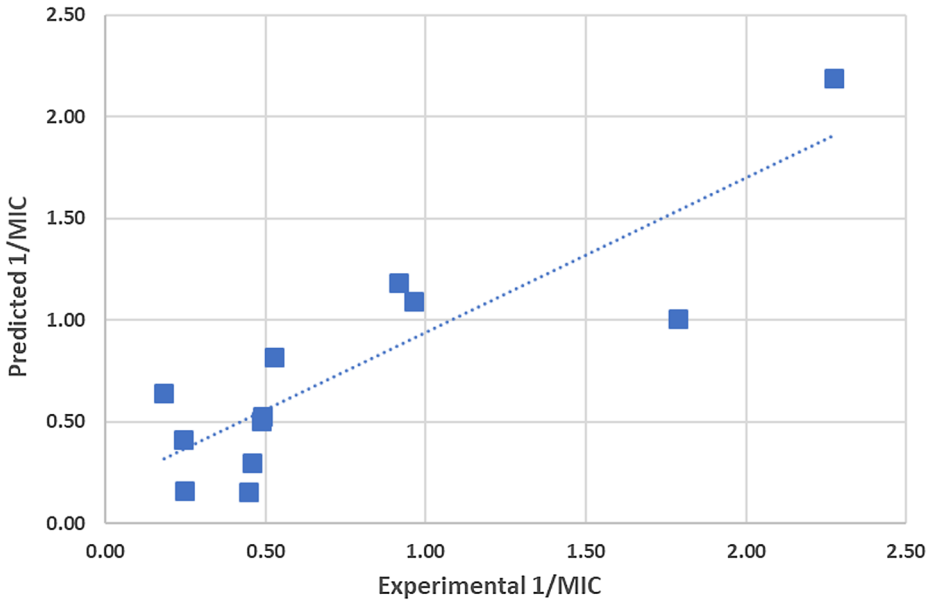

Fig. 5. Training set experimental vs. L10%OCV predicted 1/MIC.

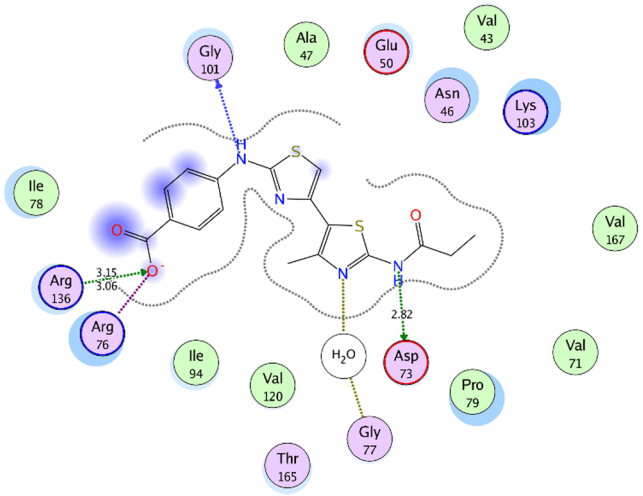

Fig. 6. 2D interaction diagram showing the thiazole inhibitor docking pose interactions with the key amino acids in the *E. coli* DNA gyrase B active site (PDB ID: 4DUH).

presence of hydrogen bond donor and acceptors on the 4-hydroxy-3-methoxyphenyl moiety increases the binding to the DNA gyrase B through the key interactions with the amino acids Asp73 and Gly77. This was confirmed by the broad-spectrum antimicrobial activity against all the tested strains (MIC: 1.02 to 8.18 μM) and the gyrase inhibitory activity (IC_{50} = 4.85 μM).

3. Conclusion

Novel 2-arylbenzothiazole hydrazides were synthesized and evaluated for their antimicrobial activity against different Gram-positive, Gram-negative bacteria and yeast, where the minimal inhibitory concentration (MIC) values were determined. Most of the tested compounds showed higher inhibitory activity against Gram-negative than against Gram-positive bacteria. The benzothiazole derivatives; *p*-hydroxy-*m*-methoxy **6c**, *p*-hydroxy **7b** and *m*-hydroxy **7c** exhibited high antibacterial activity against the most sensitive Gram-positive and Gram-negative bacteria; *E. faecalis* (*E. faecalis* MIC = 1.02, 1.04, 1.04 μM, respectively) and *K. pneumoniae* (*K. pneumoniae* MIC = 2.03, 1.04, 1.04 μM, respectively) compared to ciprofloxacin (*E. faecalis*, *K. pneumoniae* MIC = 2.93 μM). Based on the MIC values for the tested compounds against *E. coli*, compounds (**4**, **5**, **6c**, **6d**, **6g**, **6i**, **6j**, **7b**, **7c**, **7g** and **8a**) were selected and tested for their *E. coli* gyrase inhibitory activity. The selected tested compounds showed moderate inhibitory activity against *E. coli* gyrase. Moreover, compound **6c** exhibited the highest anti-gyrase activity over the other tested compounds (*E. coli* gyrase IC_{50} = 4.85 μM).The QSAR study of the tested compounds showed high correlation between the experimental and model predicted antimicrobial activity in the training set prediction and in the LOO cross-validation with predictive power R^2 of 0.810 and 0.753, respectively, and RMSE of 0.272 and 0.310, respectively. Molecular docking showed that the newly synthesized compounds possess the required structural feature for *E. coli* gyrase B inhibition through interaction with key amino acids Asp73 and Gly77.

4. Experimental protocols

4.1. Chemistry

4.1.1. General remarks

All chemicals were purchased from commercial suppliers. Analytical thin layer chromatography (TLC) was performed on precoated silica gel 60 F_{245} aluminium plates (Merck) with visualization under UV light. Melting points were determined on Electrothermal Melting Point Apparatus with open capillary tubes and uncorrected. IR spectra (4000–400 cm^{-1}) were recorded using KBr pellets using Perkin Elmer FT-IR 1650 spectrophotometer. ^{1}H- and ^{13}C NMR spectra were recorded at 400 (100) MHz using Jeol ECA 500 MHz Spectrometer and performed at Micro Analytical Laboratory Center, Faculty of Pharmacy, Cairo University, Cairo, Egypt. DMSO-d_6 was used as a solvent and chemical shifts were given in parts per million (ppm) relative to TMS as internal standard. Coupling constants were reported in Hertz (Hz). Mass spectra were measured (JEOL JMS-AX 500 Mass Spectrometer) at 70 eV. Elemental analysis, IR and mass spectra were performed at the Central Services laboratory, National Research Centre, Cairo, Egypt.

4.1.1.1. Synthesis of 4-(benzo[d]thiazol-2-yl)-2-methoxyphenol (3) [38]. A round bottomed flask with magnetic stirrer was charged with a solution of *o*-aminothiophenol **1** (2.50 g, 20 mmol) and 4-hydroxy-3-methoxybenzaldehyde **2** (3.04 g, 20 mmol) in dry dimethylformamide

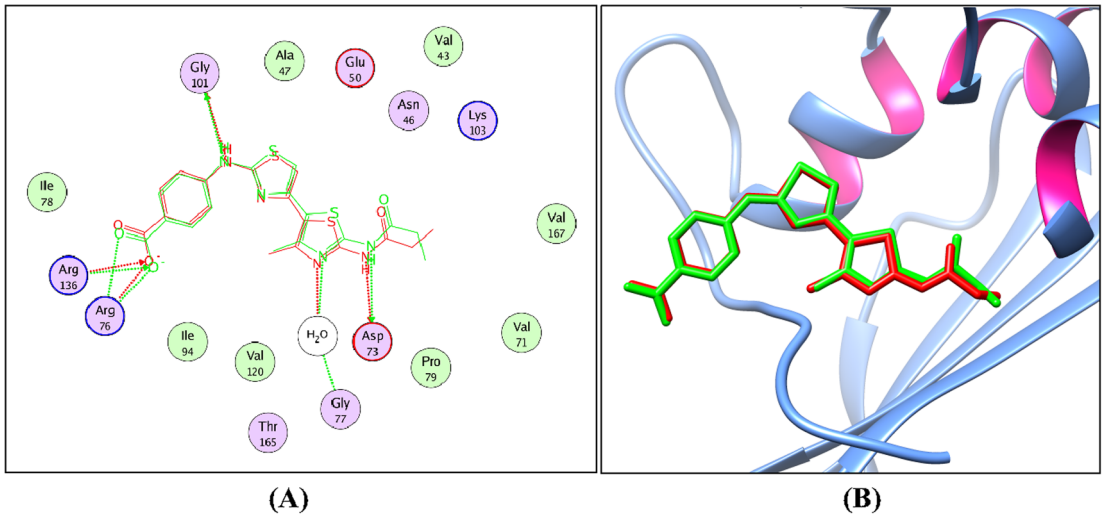

Fig. 7. 2D diagram **(A)** and 3D representation **(B)** of the superimposition of the docking pose (green) and the co-crystallized (red) of the thiazole inhibitor in the *E. coli* DNA gyrase B active site (PDB ID: 4DUH) with an RMSD of 0.432 Å.

(10 ml). The mixture was heated under reflux for 3 h. The reaction mixture was subsequently cooled to r.t. and poured over ice/water with continuous stirring. The precipitated solid was filtered and dried to give the crude product which was further purified by crystallization from methanol. Yield 76%; m.p. 168–169 °C, reported m.p. (171–173 °C) [38].

*4.1.1.2. Synthesis of ethyl 2-(4-(benzo[d]thiazol-2-yl)-2-methoxyphenoxy) propanoate (**4**).* Ethyl 2-bromopropionate ester (1.3 ml, 10 mmol) was added to a solution of 4-(benzo[*d*]thiazol-2-yl)-2-methoxyphenol **3** (2.57 g, 10 mmol) in dry dimethylformamide (10 ml) and anhydrous potassium carbonate (2.0 g, 15 mmol). The mixture was stirred and heated under reflux for 1 h, subsequently cooled to r.t. and then poured on ice/water with continuous stirring till dissolution of potassium carbonate. The precipitated solid was filtered and dried to give the crude product which was further purified by crystallization from methanol. Greyish white solid; Yield 60%; m.p. 68–69 °C; IR (KBr, cm^{-1}) 2923, 2852, 1739, 1633, 1519; ^{1}H NMR (DMSO-d_6, 400 MHz) δ: 1.18 (t, J = 7.1 Hz, 3H), 1.54 (d, J = 6.7 Hz, 3H), 3.92 (s, 3H), 4.14 (q, J = 7.1 Hz, 2H), 5.00 (q, J = 6.7 Hz, 1H), 6.95 (d, J = 8.4 Hz, 1H), 7.42 (t, J = 7.7 Hz, 1H), 7.51–7.58 (m, 2H), 7.68 (s, 1H), 8.02 (d, J = 8.1 Hz, 1H), 8.10 (d, J = 7.9 Hz, 1H) ppm; ^{13}C NMR (DMSO-d_6, 100 MHz) δ: 14.46, 18.71, 56.21, 61.37, 72.97, 110.54, 114.72, 121.11, 122.67, 123.02, 125.69, 127.03, 134.83, 149.84, 149.92, 154.03, 167.47, 171.56 ppm; MS *m/z* (%): M^+: 357.69 (100%); Anal. calcd. for $C_{19}H_{19}NO_4S$: C, 63.85; H, 5.36; N, 3.92; Found C, 63.68; H, 5.78; N, 3.75.

*4.1.1.3. Synthesis of 2-(4-(benzo[d]thiazol-2-yl)-2-methoxyphenoxy) propane hydrazide (**5**).* To a solution of ethyl propanoate compound **4** (3.57 g, 10 mmol) in absolute ethanol (20 ml), hydrazine hydrate (2 ml, 40 mmol) was added and the mixture was refluxed for 4 h. The reaction mixture was subsequently cooled to r.t. to give a solid which was collected and purified by crystallization from methanol. White solid; Yield 69%; m.p. 144–146 °C; IR (KBr, cm^{-1}): 3432, 2935, 2844, 1631, 1473; ^{1}H NMR (DMSO-d_6, 400 MHz) δ: 1.47 (d, J = 6.5 Hz, 3H), 3.92 (s, 3H), 4.32 (s, 2H), 4.77 (q, J = 6.6 Hz, 1H), 7.01 (d, J = 8.4 Hz, 1H), 7.42 (t, J = 7.4 Hz, 1H), 7.51–7.58 (m, 2H), 7.67 (s, 1H), 8.03 (d, J = 8.0 Hz, 1H), 8.10 (d, J = 7.9 Hz, 1H), 9.31 (s, 1H) ppm; ^{13}C NMR (DMSO-d_6, 100 MHz) δ: 19.23, 56.20, 74.15, 110.41, 115.14, 121.13, 122.66, 123.02, 125.69, 126.98, 127.03, 134.83, 149.98, 150.18, 154.04, 167.52, 170.15 ppm; MS *m/z* (%): M^+: 343.12 (9.22%); Anal. calcd. for $C_{17}H_{17}N_3O_3S$: C, 59.46; H, 4.99; N, 12.24; Found C, 59.68; H, 5.20; N, 12.45.

*4.1.1.4. General procedure for the synthesis of (E,Z)-2-(4-(benzo[d] thiazol-2-yl)-2-methoxyphenoxy)-N′-substituted propane hydrazides (**6a-j, 7a-i, 8a,b**).* The propane hydrazide compound **5** (1.0 g, 3.0 mmol) was refluxed with the appropriate aldehyde or ketone derivative (3.0 mmol) in absolute ethanol (10 ml) in presence of few drops of glacial acetic acid for 1 h (aldehydes or acyclic ketones) and 3 h (cyclic ketones) and the reaction was monitored by TLC. The reaction mixture was subsequently cooled to r.t. and filtered to give the crude product which was further purified by crystallization from methanol.

*4.1.1.4.1. (E,Z)-2-(4-(benzo[d]thiazol-2-yl)-2-methoxyphenoxy)-N′-benzylidene propane hydrazide (**6a**).* White solid; Yield 83%; m.p. 200–202 °C; IR (KBr) cm^{-1}: 3438, 2925, 1673, 1633; ^{1}H NMR (DMSO-d_6, 400 MHz) δ: 1.59 (d, J = 7.3 Hz, 3H), 1.61 (d, J = 7.1 Hz, 3H), 3.93 (s, 3H), 3.96 (s, 3H), 4.90 (q, J = 6.6 Hz, 1H), 5.75 (q, J = 6.6 Hz, 1H), 6.88 (d, J = 8.4 Hz, 1H), 7.06 (d, J = 8.4 Hz, 1H), 7.43–7.70 (m, 18H), 8.02–8.05 (m, 2H), 8.08 (s, 1H), 8.09–8.12 (m, 2H), 8.33 (s, 1H), 11.68 (s, 2H) ppm; ^{13}C NMR (DMSO-d_6, 100 MHz) δ: 18.13, 19.14, 56.16, 56.20, 71.04, 74.67, 110.39, 110.45, 113.66, 115.30, 121.21, 121.30, 122.62, 122.66, 122.95, 123.01, 125.64, 125.73, 126.42, 127.01, 127.05, 127.24, 127.42, 127.62, 129.30, 130.55, 130.71, 134.39, 134.46, 134.77, 134.82, 144.81, 148.74, 149.70, 149.85, 150.18, 150.35, 153.99, 154.01, 167.50, 167.64, 167.79, 172.01 ppm; MS *m/z* (%): M^+: 431.19 (39.0%), $(M+H)^+$: 432.24 (10.8%); Anal. calcd. for $C_{24}H_{21}N_3O_3S$: C, 66.80; H, 4.91; N, 9.74; Found C, 66.58; H, 4.98; N, 9.45.

*4.1.1.4.2. (E,Z)-2-(4-(benzo[d]thiazol-2-yl)-2-methoxyphenoxy)-N′-(4-hydroxybenzylidene) propane hydrazide (**6b**).* White solid; Yield 77%; m.p. > 300 °C; IR (KBr) cm^{-1}: 3436, 2927, 1671, 1608; ^{1}H NMR (DMSO-d_6, 400 MHz) δ: 1.58 (d, J = 6.2 Hz, 3H), 1.59 (d, J = 6.3 Hz, 3H), 3.93 (s, 3H), 3.96 (s, 3H), 4.87 (q, J = 6.5 Hz, 1H), 5.71 (q, J = 6.5 Hz. 1H), 6.82–6.87 (m, 5H), 7.05 (d, J = 8.4 Hz, 1H), 7.43–7.70 (m, 12H), 7.97 (s, 1H), 8.03–8.12 (m, 4H), 8.21 (s, 1H), 9.98 (br s, 2H), 11.46 (s, 2H) ppm; ^{13}C NMR (DMSO-d_6, 100 MHz) δ: 18.11, 19.19, 56.14, 56.18, 70.98, 74.68, 110.36, 110.43, 113.53, 115.24, 116.19, 121.20, 121.29, 122.59, 122.63, 122.94, 123.00, 125.42, 125.62, 125.71, 126.34, 126.99, 127.03, 127.19, 129.17, 129.44, 134.78, 134.82, 145.11, 149.01, 149.66, 149.88, 150.15, 150.40, 153.99, 154.01, 159.86, 160.02, 167.41, 167.52, 167.66, 171.65 ppm; Anal. calcd. for $C_{24}H_{21}N_3O_4S$: C, 64.42; H, 4.73; N, 9.39 Found C, 64.58; H, 4.58; N, 9.45.

*4.1.1.5. (E,Z)-(2-(4-(benzo[d]thiazol-2-yl)-2-methoxyphenoxy)-N′-(4-hydroxy-3-methoxybenzylidene) propane hydrazide (**6c**).* White solid; Yield 90%; m.p. > 300 °C; IR (KBr) cm^{-1}: 3438, 2925, 1650, 1600; ^{1}H NMR

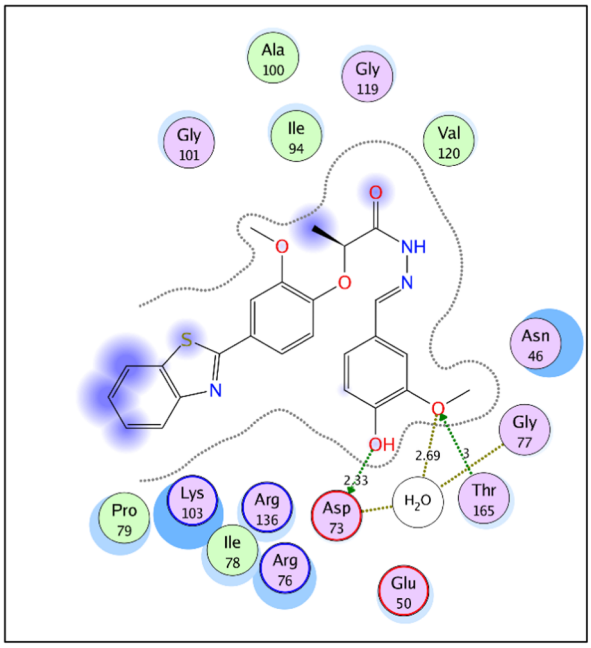

(A)

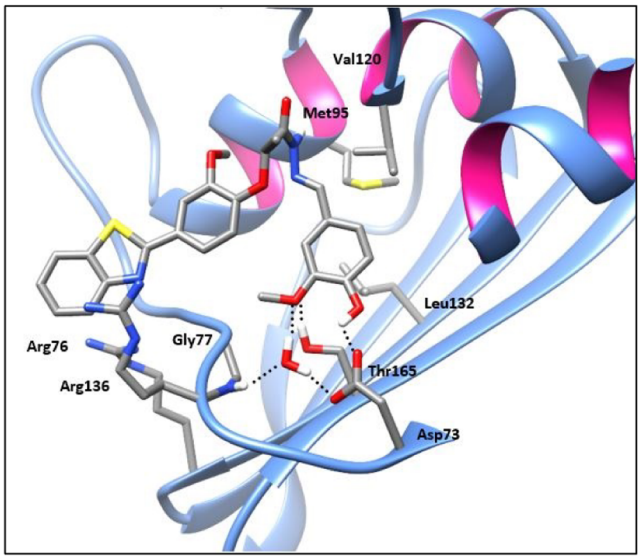

(B)

Fig. 8. 2D diagram **(A)** and 3D representation **(B)** of compound **6c** showing its interaction with the *E. coli* DNA gyrase B active site.

(DMSO-d_6, 400 MHz) δ: 1.58 (d, J = 5.9 Hz, 3H), 1.59 (d, J = 5.6 Hz, 3H), 3.78 (s, 3H), 3.81 (s, 3H), 3.92 (s, 3H), 3.96 (s, 3H), 4.87 (q, J = 6.5 Hz, 1H), 5.75 (q, J = 6.6 Hz, 1H), 6.82 (d, J = 8.4 Hz, 1H), 6.89 (d, J = 8.4 Hz, 1H), 7.04–7.70 (m, 14H), 7.94 (s, 1H), 8.03–8.05 (m, 2H), 8.10–8.12 (m, 2H), 8.19 (s, 1H), 9.59 (br s, 1H), 9.62 (br s, 1H), 11.48 (s, 2H) ppm; ^{13}C NMR (DMSO-d_6, 100 MHz) δ: 17.99, 19.23, 55.98, 56.03, 56.17, 56.20, 70.92, 74.68, 109.39, 110.14, 110.38, 110.44, 113.53, 115.24, 115.89, 116.06, 121.22, 121.33, 121.82, 122.67, 122.79, 122.96, 123.03, 125.61, 125.69, 126.32, 127.02, 127.18, 134.80, 134.85, 145.11, 148.47, 148.54, 149.18, 149.67, 149.95, 150.17, 150.42, 154.03, 154.06, 167.32, 167.49, 167.62, 171.58 ppm; MS m/z (%): M^+: 477.01 (0.79%); Anal. calcd. for $C_{25}H_{23}N_3O_5S$: C, 62.88; H, 4.85; N, 8.80; Found C, 62.58; H, 4.58; N, 8.45.

4.1.1.5.1. (E,Z)-2-(4-(benzo[d]thiazol-2-yl)-2-methoxyphenoxy)-N′-(4-fluorobenzylidene) propane hydrazide ***(6d)***. White solid; Yield 54%; m.p. 160–162 °C; IR (KBr) cm^{-1}: 3432, 2923, 1677, 1608; ^{1}H NMR (DMSO-d_6, 400 MHz) δ: 1.57 (d, J = 6.5 Hz, 3H), 1.59 (d, J = 6.5 Hz, 3H), 3.92 (s, 3H), 3.95 (s, 3H), 4.89 (q, J = 6.6 Hz, 1H), 5.73 (q, J = 6.6 Hz, 1H), 6.86 (d, J = 8.5 Hz, 1H), 7.04 (d, J = 8.5 Hz, 1H), 7.25.-7.31 (m, 4H), 7.40–7.47 (m, 2H), 7.51–7.61 (m, 4H), 7.67–7.77 (m, 6H), 8.01–8.12 (m, 5H), 8.32 (s, 1H), 11.66 (s, 1H), 11.67 (s, 1H) ppm; MS m/z (%): M^+: 449.27 (24.9%), $(M+H)^+$: 450.55 (7.0%); Anal. calcd. for $C_{24}H_{20}$ FN_3O_3S: C, 64.13; H, 4.48; N, 9.35; Found C, 64.48; H, 4.58; N, 9.65.

4.1.1.5.2. (E,Z)-2-(4-(Benzo[d]thiazol-2-yl)-2-methoxyphenoxy)-N′-(4-chloro-3-nitrobenzylidene) propane hydrazide ***(6e)***. Yellow solid; Yield 91%; m.p. 170–173 °C; IR (KBr) cm^{-1}: 3434, 2922, 1668, 1530, 1350; ^{1}H NMR (DMSO-d_6, 400 MHz) δ: 1.58 (d, J = 6.5 Hz, 3H), 1.60 (d, J = 6.5 Hz, 3H), 3.91 (s, 3H), 3.95 (s, 3H), 4.90 (q, J = 6.6 Hz, 1H), 5.79 (q, J = 6.6 Hz, 1H), 6.88 (d, J = 8.4 Hz, 1H), 7.04 (d, J = 8.4 Hz, 1H), 7.40–7.61 (m, 6H), 7.66–7.71 (m, 2H), 7.79–7.85 (m, 2H), 8.01–8.17 (m, 5H), 8.35–8.39 (m, 3H), 8.55 (s, 1H), 8.81 (s, 1H), 11.88 (s, 1H), 11.91 (s, 1H) ppm; ^{13}C NMR (DMSO-d_6, 100 MHz) δ: 18.18, 19.05, 56.15, 56.19, 71.02, 74.69, 110.38, 110.46, 113.85, 115.32, 121.18, 121.25, 122.60, 122.95, 123.02, 123.65, 124.14, 125.55, 125.71, 125.90, 126.42, 126.50, 127.02, 127.33, 131.86, 132.05, 132.41, 132.65, 132.94, 133.36, 134.79, 134.83, 135.12, 135.18, 141.42, 145.30, 148.27, 148.56, 149.72, 149.77, 150.18, 150.27, 154.00, 159.98, 167.44, 167.57, 168.18; 172.38 ppm; Anal. Calcd for $C_{24}H_{19}ClN_4O_5S$: C, 56.42; H, 3.75; N, 10.97. Found: C, 56.66; H, 3.80; N, 10.90.

4.1.1.5.3. (E,Z)-2-(4-(benzo[d]thiazol-2-yl)-2-methoxyphenoxy)-N′-(4-nitrobenzylidene) propane hydrazide ***(6f)***. Yellowish white solid; Yield 79%; m.p. 190–192 °C; IR (KBr) cm^{-1}: 3442, 2925, 1685, 1631, 1519, 1349; ^{1}H NMR (DMSO-d_6, 400 MHz) δ: 1.60 (d, J = 6.5 Hz, 3H), 1.62 (d, J = 6.5 Hz, 3H), 3.92 (s, 3H), 3.96 (s, 3H), 4.91 (q, J = 6.6 Hz, 1H), 5.76 (q, J = 6.6 Hz, 1H), 6.89 (d, J = 8.5 Hz, 1H), 7.05 (d, J = 8.5 Hz, 1H), 7.41–7.44 (m, 2H), 7.51–7.61 (m, 4H), 7.66–7.71 (m, 2H), 7.95–7.97 (m, 3H), 8.01–8.12 (m, 3H), 8.16 (s, 1H); 8.24–8.30 (m, 4H), 8.43 (s, 1H), 11.97 (s, 2H) ppm; ^{13}C NMR (DMSO-d_6, 100 MHz) δ: 18.13, 19.04, 56.17, 56.20, 71.20, 74.68, 110.42, 110.47, 113.95, 115.37, 121.19, 121.27, 122.60, 122.64, 122.93, 122.99, 124.42, 124.47, 125.68, 125.76, 126.55, 127.03, 127.07, 127.32, 128.35, 128.58, 134.74, 134.79, 140.62, 140.71, 142.48, 146.39, 148.23, 148.42, 149.72, 149.76, 150.18, 150.28, 153.96, 167.50, 167.61, 168.34, 172.42 ppm; MS m/z (%): M^+: 476.19 (12.2%), $(M+H)^+$: 477.24 (3.2%); Anal. calcd. for $C_{24}H_{20}N_4O_5S$: C, 60.49; H, 4.23; N, 11.76; Found C, 60.58; H, 4.58; N, 11.45.

4.1.1.5.4. (E,Z)-2-(4-(Benzo[d]thiazol-2-yl)-2-methoxyphenoxy)-N′-(4-cyanobenzylidene) propane hydrazide ***(6g)***. White solid; Yield 90%; m.p. 157–159 °C; IR (KBr) cm^{-1}: 3435, 3203, 2923, 2226, 1678, 1645; ^{1}H NMR (DMSO-d_6, 400 MHz) δ: 1.58 (d, J = 6.5 Hz, 3H), 1.61 (d, J = 6.5 Hz, 3H), 3.92 (s, 3H), 3.95 (s, 3H), 4.92 (q, J = 6.6 Hz, 1H), 5.78 (q, J = 6.5 Hz, 1H), 6.88 (d, J = 8.4 Hz, 1H), 7.05 (d, J = 8.4 Hz, 1H), 7.43–8.12 (m, 20H), 8.38 (s, 1H), 8.79 (s, 1H), 11.88 (s, 1H), 11.91 (s, 1H) ppm; ^{13}C NMR (DMSO-d_6, 100 MHz) δ: 18.23, 19.07, 56.17, 56.20, 71.07, 74.70, 110.40, 110.46, 112.33, 112.51, 113.79, 115.32, 119.07, 119.12, 121.21, 121.30, 122.64, 122.97, 122.68, 123.04, 125.63, 125.71, 126.50, 126.67, 126.73, 126.99, 127.03, 127.31, 128.03, 128.17, 133.17, 133.19, 134.80, 134.85, 138.86, 138.99, 142.85, 146.76, 149.72, 149.80, 150.20, 150.28, 154.02, 154.05, 167.45, 167.58, 168.09, 172.35 ppm; Anal. Calcd for $C_{25}H_{20}N_4O_3S$: C, 65.77; H, 4.42; N, 12.27. Found: C, 65.17; H, 4.50; N, 12.27.

4.1.1.5.5. (E,Z)-2-(4-(benzo[d]thiazol-2-yl)-2-methoxyphenoxy)-N′-((2-(thiophen-2-yl)-1H-indol-3-yl)methylene) propane hydrazide ***(6h)***. Dark violet solid; Yield 90%; m.p. 180–182 °C; IR (KBr) cm^{-1}: 3432, 2925, 1664, 1608; ^{1}H NMR (DMSO-d_6, 400 MHz) δ: 1.61 (d, J = 6.4 Hz, 3H), 1.69 (d, J = 6.4 Hz, 3H), 3.95 (s, 3H), 3.96 (s, 3H),

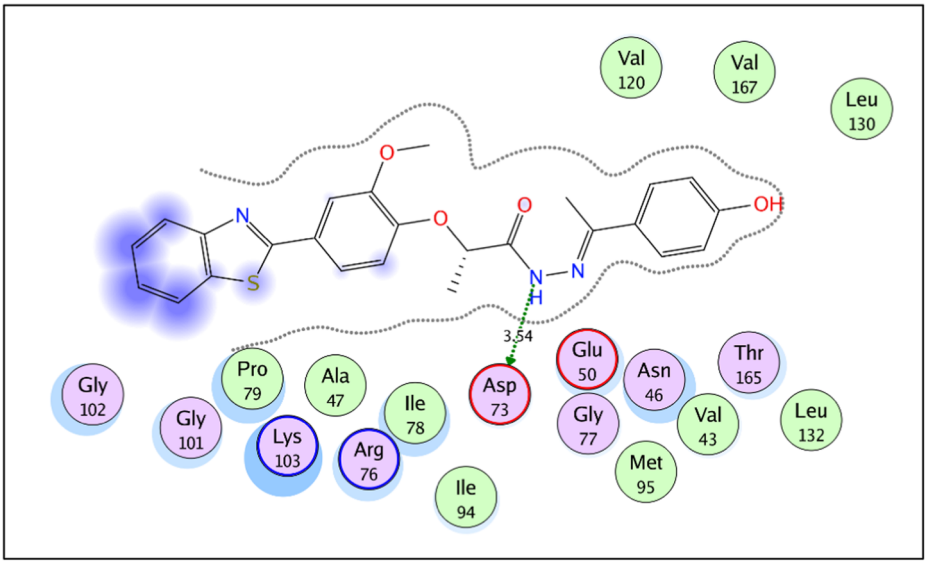

(A)

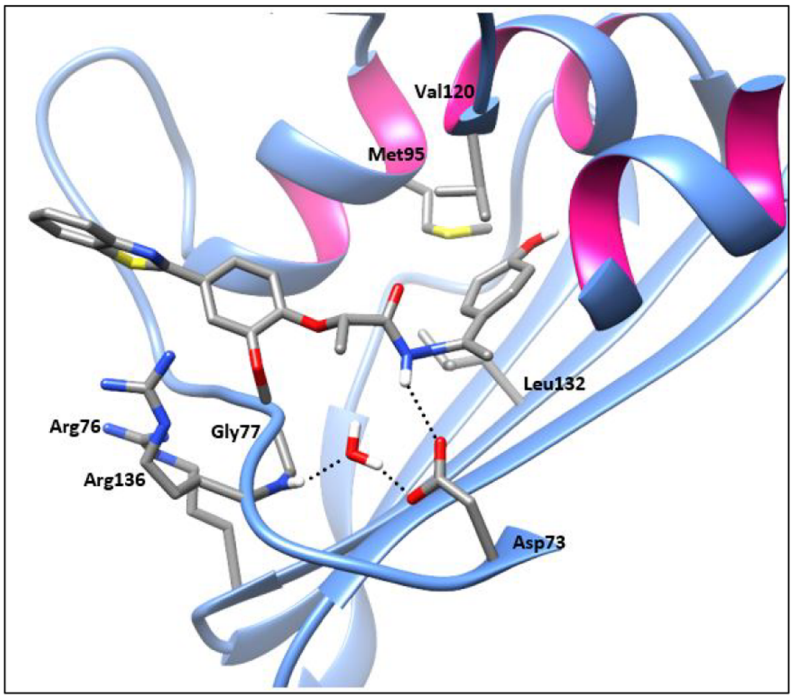

(B)

Fig. 9. 2D diagram **(A)** and 3D representation **(B)** of compound **7b** showing its interaction with the *E. coli* DNA gyrase B active site.

4.88 (q, J = 6.6 Hz, 1H), 5.80 (q, J = 6.6 Hz, 1H), 6.90 (d, J = 8.5 Hz, 1H), 7.08 (d, J = 8.5 Hz, 1H), 7.15–7.31 (m, 6H), 7.42–7.60 (m, 10*H*), 7.70–7.85 (m, 4H), 8.02–8.07 (m, 4H), 8.17 (d, J = 7.8 Hz, 1H), 8.37 (d, J = 7.8 Hz, 1H), 8.65 (s, 1H), 8.81 (s, 1H), 11.44 (s, 1H), 11.53 (s, 1H), 11.89 (s, 1H), 11.93 (s, 1H) ppm; Anal. calcd. for $C_{30}H_{24}N_4O_3S_2$: C, 65.20; H, 4.38; N, 10.14; Found C, 65.58; H, 4.58; N, 10.35.

*4.1.1.5.6. (E,Z)-2-(4-(benzo[d]thiazol-2-yl)-2-methoxyphenoxy)-N′-((5-methylfuran-2-yl)methylene) propane hydrazide (**6i**).* White solid; Yield 88%; m.p. 190–192 °C; IR (KBr) cm^{-1}: 3432, 2929, 1658, 1581; ^{1}H NMR (DMSO-d_6, 400 MHz) δ: 1.56 (d, J = 6.2 Hz, 3H), 1.57 (d, J = 6.3 Hz, 3H), 2.32 (s, 3H), 2.34 (s, 3H), 3.92 (s, 3H), 3.94 (s, 3H), 4.85 (q, J = 6.6 Hz, 1H), 5.59 (q, J = 6.5 Hz, 1H), 6.25 (d, J = 3.2 Hz, 2H), 6.79 (d, J = 8.5 Hz, 1H), 6.83 (d, J = 7.1 Hz, 1H), 7.03 (d, J = 8.3 Hz, 1H), 7.43–7.70 (m, 9H), 7.88 (s, 1H), 8.03–8.11 (m, 5H), 11.53 (s, 2H) ppm; Anal. calcd. for $C_{23}H_{21}N_3O_4S$: C, 63.43; H, 4.86; N, 9.65; Found C, 63.28; H, 4.98; N, 9.85.

*4.1.1.5.7. (E,Z)-2-(4-(Benzo[d]thiazol-2-yl)-2-methoxyphenoxy)-N′-((1,5-dimethyl-3-oxo-2-phenyl-2,3-dihydro-1H-pyrazol-4-yl)methylene) propane hydrazide (**6j**).* White solid; Yield 78%; m.p. 166–169 °C; IR (KBr) cm^{-1}: 3434, 2927, 1636; ^{1}H NMR (DMSO-d_6, 400 MHz) δ: 1.53 (d, J = 8.3 Hz, 3H), 1.58 (d, J = 8.3 Hz, 3H), 2.43 (s, 3H), 2.56 (s, 3H), 3.26 (s, 3H), 3.28 (s, 3H), 3.81 (s, 3H), 3.93 (s, 3H), 4.76 (q, J = 6.6 Hz,

Table 6
Docking energy scores (*S*) in kcal/mol for the synthesized compounds **3–8** in DNA gyrase B active site.

Compound No.	Energy score (S) kcal/mol	Compound No.	Energy score (S) kcal/mol
3	−11.73	**6j**	−12.82
4	−13.23	**7a**	−12.57
5	−11.30	**7b**	−12.45
6a	−13.04	**7c**	−11.95
6b	−14.47	**7d**	−13.28
6c	−16.17	**7e**	−12.69
6d	−14.72	**7g**	−12.66
6e	−12.08	**7h**	−12.10
6f	−12.93	**7i**	−12.68
6g	−13.15	**8a**	−13.87
6h	−16.99	**8b**	−14.52
6i	−12.38	**Co-crystalized ligand**	−14.46

1H), 5.60 (q, *J* = 6.6 Hz, 1H), 6.76 (d, *J* = 8.4 Hz, 1H), 6.93 (d, *J* = 8.2 Hz, 1H), 7.05 (d, *J* = 8.4 Hz, 1H), 7.34–7.69 (m, 17H), 7.92 (s, 1H), 8.02–8.05 (m, 2H), 8.10 (s, 1H), 8.09–8.12 (m, 2H), 11.30 (s, 2H) ppm; Anal. calcd. for $C_{29}H_{27}N_5O_4S$: C, 64.31; H, 5.02; N, 12.93; Found C, 64.41; H, 5.22; N, 12.95.

*4.1.1.5.8. (E,Z)-2-(4-(benzo[d]thiazol-2-yl)-2-methoxyphenoxy)-N′-(1-phenylethylidene) propane hydrazide (**7a**)*. White solid; Yield 85%; m.p. 131–133 °C; IR (KBr, cm^{-1}): 3424, 2925, 2859, 1668, 1598; ^{1}H NMR (DMSO-d_6, 400 MHz) *δ*: 1.60 (d, *J* = 4.2 Hz, 3H), 1.62 (d, *J* = 2.1 Hz, 3H), 2.32 (s, 3H), 2.33 (s, 3H), 3.93 (s, 3H), 3.96 (s, 3H), 5.14 (q, *J* = 6.4 Hz, 1H), 5.75 (q, *J* = 6.4 Hz, 1H), 6.84 (d, *J* = 8.4 Hz, 1H), 7.09 (q, *J* = 8.4 Hz, 1H), 7.42–7.50 (m, 8H), 7.52–7.60 (m, 4H), 7.67–7.71 (m, 2H), 7.80–7.82 (m, 4H), 8.02–8.12 (m, 4H), 10.60 (s, 1H), 10.89 (s, 1H) ppm; ^{13}C NMR (DMSO-d_6, 100 MHz) *δ*: 14.12, 14.53, 18.18, 19.28, 56.13, 56.25, 71.31, 73.83, 110.31, 110.40, 113.57, 114.81, 121.25, 121.31, 122.65, 122.94, 122.99, 125.65, 125.73, 126.33, 126.59, 126.87, 127.01, 128.83, 128.92, 129.75, 129.99, 134.76, 134.90, 138.37, 138.46, 149.50, 149.64, 149.83, 150.01, 150.38, 154.00, 154.27, 167.54, 167.66, 167.82, 172.83 ppm; MS *m/z* (%): M^+: 445.19 (22.5%), $(M+H)^+$: 446.24 (6.5%); Anal. calcd. for $C_{25}H_{23}N_3O_3S$: C, 67.40; H, 5.23; N, 9.43; Found C, 67.35; H, 5.19; N, 9.55.

*4.1.1.5.9. (E,Z)-2-(4-(benzo[d]thiazol-2-yl)-2-methoxyphenoxy)-N′-(1-(4-hydroxyphenyl)ethylidene) propane hydrazide (**7b**)*. White solid; Yield 83%; m.p. 247–248 °C; IR (KBr, cm^{-1}): 3420, 3340 3058, 2927, 1671, 1614, 1513; ^{1}H NMR (DMSO-d_6, 400 MHz) *δ*: 1.59 (d, *J* = 6.2 Hz, 6H), 2.25 (s, 6H), 3.93 (s, 3H), 3.95 (s, 3H), 5.11 (q, *J* = 6.5 Hz, 1H), 5.74 (q, *J* = 6.6 Hz, 1H), 6.78 (d, *J* = 8.6 Hz, 4H), 6.82 (d, *J* = 8.5 Hz, 1H), 7.09 (d, *J* = 8.4 Hz, 1H), 7.42–7.44 (m, 2H), 7.52–7.70 (m, 10H), 8.01–8.03 (m, 2H), 8.04–8.10 (m, 2H), 9.81 (s, 2H), 10.46 (s, 1H), 10.72 (s, 1H) ppm; ^{13}C NMR (DMSO-d_6, 100 MHz) *δ*: 13.90, 14.26, 18.11, 19.28, 56.11, 56.23, 71.28, 73.96, 110.27, 110.37, 113.50, 114.82, 115.57, 115.67, 121.23, 122.62, 122.71, 122.90, 122.95, 125.67, 125.75, 126.26, 126.98, 127.08, 128.19, 128.55, 129.03, 129.25, 134.72, 134.76, 149.60, 149.79, 149.98, 150.38, 153.93, 154.95, 159.10, 159.34, 167.55, 167.60, 167.65, 172.59 ppm; MS *m/z* (%): M^+: 461.93 (18.26%); Anal. calcd. for $C_{25}H_{23}N_3O_4S$: C, 65.06; H, 5.02; N, 9.10; Found C, 65.26; H, 5.13; N, 9.20.

*4.1.1.5.10. (E,Z)-2-(4-(benzo[d]thiazol-2-yl)-2-methoxyphenoxy)-N′-(1-(3-hydroxyphenyl) ethylidene) propane hydrazide (**7c**)*. White solid; Yield 91%; m.p. 248–250 °C; IR (KBr, cm^{-1}): 3430, 2973, 2923, 1666, 1621; ^{1}H NMR (DMSO-d_6, 400 MHz) *δ*: 1.59 (d, *J* = 6.4 Hz, 6H), 2.25 (s, 6H), 3.93 (s, 3H), 3.95 (s, 3H), 5.10 (q, *J* = 6.5 Hz, 1H), 5.73 (q, *J* = 6.5 Hz, 1H), 6.78 (d, *J* = 8.7 Hz, 4H), 6.82 (d, *J* = 8.5 Hz, 1H), 7.09 (d, *J* = 8.4 Hz, 1H), 7.40–7.44 (m, 2H), 7.51–7.62 (m, 4H), 7.65–7.71 (m, 6H), 8.01–8.04 (m, 2H), 8.08–8.11 (m, 2H), 9.77 (s, 2H), 10.45 (s, 1H), 10.73 (s, 1H) ppm; ^{13}C NMR (DMSO-d_6, 100 MHz) *δ*: 13.92, 14.28, 18.15, 19.29, 56.13, 56.25, 71.27, 73.97, 110.30, 110.40, 113.54, 114.80, 115.56, 115.65, 121.24, 122.64, 122.98, 125.64, 125.78, 126.28, 126.99, 127.07, 128.18, 128.53, 129.07, 129.28, 134.79, 134.87, 149.56, 149.63, 149.78, 149.90, 150.41, 153.99, 154.67, 155.02, 159.11, 159.34, 167.50, 167.55, 167.65, 172.57 ppm; Anal. calcd. for $C_{25}H_{23}N_3O_4S$: C, 65.06; H, 5.02; N, 9.10; Found C, 65.07; H, 5.22; N, 9.18.

*4.1.1.5.11. (E,Z)-2-(4-(benzo[d]thiazol-2-yl)-2-methoxyphenoxy)-N′-(1-(4-methoxyphenyl)ethylidene) propane hydrazide (**7d**)*. White solid; Yield 90%; m.p. 197–198 °C; IR (KBr, cm^{-1}): 3432, 3203, 3091, 2923, 1677, 1604; ^{1}H NMR (DMSO-d_6, 400 MHz) *δ*: 1.60 (d, *J* = 5.2 Hz, 6H), 2.28 (s, 6H), 3.77 (s, 3H), 3.79 (s, 3H), 3.93 (s, 3H), 3.95 (s, 3H), 5.13 (q, *J* = 6.2 Hz, 1H), 5.75 (q, *J* = 6.2 Hz, 1H), 6.84–7.12 (m, 6H), 7.42–7.43 (m, 2H), 7.52–7.62 (m, 4H), 7.67–7.77 (m, 6H), 8.03–8.10 (m, 4H), 10.53 (s, 1H), 10.77 (s, 1H) ppm; ^{13}C NMR (DMSO-d_6, 100 MHz) *δ*: 13.95, 14.32, 18.12, 19.28, 55.62, 55.65, 56.11, 56.22, 71.37, 73.91, 110.30, 110.37, 113.58, 114.15, 114.22, 114.80, 121.23, 121.28, 122.62, 122.70, 122.90, 122.97, 125.64, 125.72, 126.32, 127.01, 127.09, 128.07, 128.43, 130.59, 130.78, 134.74, 134.78, 149.38, 149.64, 149.81, 149.98, 150.43, 153.97, 154.36, 160.66, 160.87, 167.56, 167.66, 167.78, 172.63 ppm; Anal. calcd. for $C_{26}H_{25}N_3O_4S$: C, 65.67; H, 5.30; N, 8.84; Found C, 65.87; H, 5.40; N, 8.64.

*4.1.1.5.12. (E,Z)-2-(4-(benzo[d]thiazol-2-yl)-2-methoxyphenoxy)-N′-(1-(4-chlorophenyl)ethylidene) propane hydrazide (**7e**)*. White solid; Yield 84%; m.p. 214–215 °C; IR (KBr, cm^{-1}): 3423, 3199, 3093, 2927, 1679, 1598; ^{1}H NMR (DMSO-d_6, 400 MHz) *δ*: 1.59 (d, *J* = 6.4 Hz, 6H), 2.30 (s, 3H), 2.32 (s, 3H), 3.92 (s, 3H), 3.95 (s, 3H), 5.16 (q, *J* = 6.5 Hz, 1H), 5.76 (q, *J* = 6.6 Hz, 1H), 6.84 (d, *J* = 8.4 Hz, 1H), 7.08 (d, *J* = 8.4 Hz, 1H), 7.45–7.59 (m, 10*H*), 7.67 (d, *J* = 15.2 Hz, 2H), 7.81 (d, *J* = 6.0 Hz, 4H), 8.01–8.11 (m, 4H), 10.65 (s, 1H), 10.94 (s, 1H) ppm; ^{13}C NMR (DMSO-d_6, 100 MHz) *δ*: 13.98, 14.38, 18.93, 19.26, 56.13, 56.24, 71.38, 73.78, 110.31, 110.39, 113.67, 114.80, 121.24, 121.28, 122.61, 122.64, 122.93, 122.98, 125.65, 125.73, 126.37, 127.01, 127.06, 128.36, 128.64, 128.85, 128.87, 134.42, 134.75, 137.09, 137.17, 148.35, 149.65, 149.80, 149.99, 150.36, 152.99, 153.96, 167.54, 167.65, 167.96, 172.87 ppm; MS *m/z* (%): M^+: 478.96 (4.2%), $(M+H)^+$: 480.00 (1.9%); Anal. calcd. for $C_{25}H_{22}ClN_3O_3S$: C, 62.56; H, 4.62; N, 8.75; Found C, 62.37; H, 4.44; N, 8.85.

*4.1.1.5.13. (E,Z)-2-(4-(benzo[d]thiazol-2-yl)-2-methoxyphenoxy)-N′-(1-(4-bromophenyl)ethylidene) propane hydrazide (**7f**)*. White solid; Yield 78%; m.p. 194–195 °C; IR (KBr, cm^{-1}): 3430, 3261, 2929, 2859, 1679, 1598; ^{1}H NMR (DMSO-d_6, 400 MHz) *δ*: 1.59 (d, *J* = 6.4 Hz, 6H), 2.29 (s, 3H), 2.31 (s, 3H), 3.92 (s, 3H), 3.95 (s, 3H), 5.16 (q, *J* = 6.6 Hz, 1H), 5.76 (q, *J* = 6.9 Hz, 1H), 6.84 (d, *J* = 8.4 Hz, 1H), 7.08 (d, *J* = 8.3 Hz, 1H), 7.39–7.43 (m, 2H), 7.51–7.67 (m, 10H), 7.74–7.75 (m, 4H), 8.02–8.11 (m, 4H), 10.69 (s, 1H), 10.92 (s, 1H) ppm; ^{13}C NMR (DMSO-d_6, 100 MHz) *δ*: 13.93, 14.33, 18.14, 19.25, 56.13, 56.24, 71.40, 73.77, 110.31, 110.39, 113.71, 114.80, 121.28, 121.32, 122.60, 122.65, 122.92, 122.95, 125.70, 125.76, 126.37, 127.05, 127.09, 128.64, 128.92, 131.80, 131.89, 134.77, 134.84, 137.52, 137.61, 148.49, 149.65, 149.78, 149.98, 150.36, 153.16, 153.95, 167.58, 167.68, 168.03, 172.88 ppm; Anal. calcd. for $C_{25}H_{22}BrN_3O_3S$: C, 57.26; H, 4.23; N, 8.01; Found C, 57.28; H, 4.43; N, 8.13.

*4.1.1.5.14. (E,Z)-2-(4-(benzo[d]thiazol-2-yl)-2-methoxyphenoxy)-N′-(1-(4-nitrophenyl)ethylidene) propane hydrazide (**7g**)*. Yellow solid; Yield 76%; m.p 207–208 °C; IR (KBr, cm^{-1}): 3425, 3199, 3095, 2925, 1683, 1592, 1508, 1334; ^{1}H NMR (DMSO-d_6, 400 MHz) *δ*: 1.61 (d, *J* = 6.5 Hz, 6H), 2.36 (s, 3H), 2.39 (s, 3H), 3.92 (s, 3H), 3.96 (s, 3H), 5.20 (q, *J* = 6.4 Hz, 1H), 5.80 (q, *J* = 6.6 Hz, 1H), 6.87 (d, *J* = 8.4 Hz, 1H), 7.08 (d, *J* = 8.4 Hz, 1H), 7.41–7.42 (m, 2H), 7.44–7.55 (m, 4H), 7.59–7.71 (m, 2H), 8.01–8.11 (m, 8H), 8.21–8.28 (m, 4H), 10.84 (s, 1H), 11.11 (s, 1H) ppm; ^{13}C NMR (DMSO-d_6, 100 MHz) *δ*: 14.01, 14.45, 18.14, 19.22, 56.11, 56.22, 71.52, 73.73, 110.30, 110.38, 113.81, 114.80, 121.23,

121.29, 122.56, 122.60, 122.91, 122.96, 123.94, 125.64, 125.72, 126.45, 127.01, 127.04, 127.67, 128.00, 134.73, 134.77, 144.37, 147.33, 147.85, 148.09, 149.68, 149.74, 149.98, 150.35, 151.70, 153.95, 167.52, 167.60, 168.34, 173.11 ppm; Anal. calcd. for $C_{25}H_{22}N_4O_5S$: C, 61.21; H, 4.52; N, 11.42; Found C, 61.31; H, 4.32; N, 11.63.

*4.1.1.5.15. (E,Z)-2-(4-(benzo[d]thiazol-2-yl)-2-methoxyphenoxy)-N′-(1-(thiophen-2-yl)ethylidene) propane hydrazide (**7h**).* White solid; Yield 73%; m.p. 196–197 °C; IR (KBr, cm^{-1}): 3432, 2973, 2925, 1660, 1631, 1558; ^{1}H NMR (DMSO-d_6, 400 MHz) δ: 1.58–1.61 (m, 6H), 2.33 (s, 6H), 3.93 (s, 3H), 3.95 (s, 3H), 5.11 (q, J = 6.4 Hz, 1H), 5.63 (q, J = 6.4 Hz, 1H), 6.81 (d, J = 8.4 Hz, 1H), 7.08–7.10 (m, 3H), 7.43–7.61 (m, 10H), 7.68 (d, J = 6.6 Hz, 2H), 8.02–8.12 (m, 4H), 10.58 (s, 1H), 10.82 (s, 1H) ppm; ^{13}C NMR (DMSO-d_6, 100 MHz) δ: 14.37, 14.87, 18.12, 19.25, 56.14, 56.24, 71.23, 73.77, 110.35, 110.39, 113.62, 114.81, 121.24, 122.64, 122.92, 122.97, 125.76, 125.80, 126.43, 127.03, 127.08, 128.09, 128.16, 128.25, 128.94, 129.60, 134.77, 143.25, 143.75, 146.02, 149.67, 149.79, 149.98, 150.24, 151.23, 153.94, 167.52, 167.58, 167.67, 172.47 ppm; MS m/z (%): M^+: 450.95 (1.7%); Anal. calcd. for $C_{23}H_{21}N_3O_3S_2$: C, 61.18; H, 4.69; N, 9.31; Found C, 61.28; H, 4.70; N, 9.21.

*4.1.1.5.16. (E,Z)-2-(4-(benzo[d]thiazol-2-yl)-2-methoxyphenoxy)-N′-(1-(furan-2-yl)ethylidene) propane hydrazide (**7i**).* White solid; Yield 82%; m.p. 216–217 °C; IR (KBr, cm^{-1}): 3440, 2925, 2861, 1670, 1596; ^{1}H NMR (DMSO-d_6, 400 MHz) δ: 1.58 (d, J = 6.4 Hz, 6H), 2.24 (s, 6H), 3.93 (s, 3H), 3.95 (s, 3H), 5.11 (q, J = 6.5 Hz, 1H), 5.67 (q, J = 6.6 Hz, 1H), 6.60 (d, J = 3 Hz, 2H), 6.83 (d, J = 8.4 Hz, 1H), 6.97 (d, J = 3 Hz, 2H), 7.07 (d, J = 8.2 Hz, 1H), 7.43–7.45 (m, 2H), 7.51–7.61 (m, 4H), 7.67 (d, J = 11.2 Hz, 2H), 7.78–7.80 (m, 2H), 8.02–8.12 (m, 4H), 10.53 (s, 1H), 10.85 (s, 1H) ppm; ^{13}C NMR (DMSO-d_6, 100 MHz) δ: 13.63, 13.92, 18.21, 19.25, 56.12, 56.23, 71.06, 73.75, 110.30, 110.38, 111.62, 112.40, 112.46, 113.52, 114.79, 116.41, 121.23, 121.29, 122.61, 122.66, 122.94, 122.99, 125.69, 125.74, 126.34, 126.97, 127.07, 134.75, 134.79, 141.65, 144.95, 145.24, 146.08, 149.62, 149.79, 149.98, 150.30, 151.91, 153.97, 167.55, 167.70, 172.68 ppm; Anal. calcd. for $C_{23}H_{21}N_3O_4S$: C, 63.43; H, 4.86; N, 9.65; Found C, 63.53; H, 4.45; N, 9.78.

*4.1.1.5.17. 2-(4-(Benzo[d]thiazol-2-yl)-2-methoxyphenoxy)-N′-(2-oxoindolin-3-ylidene) propane hydrazide (**8a**).* Yellowish white solid; Yield 78%; m.p. 162–165 °C; IR (KBr, cm^{-1}): 3432, 2935, 1716, 1631; ^{1}H NMR (DMSO-d_6, 400 MHz) δ: 1.59 (d, J = 6.4 Hz, 3H), 3.97 (s, 3H), 5.17 (q, J = 6.5 Hz, 1H), 6.93 (d, J = 8.5 Hz, 1H), 7.09 (t, J = 8.4 Hz, 1H), 7.23 (d, J = 8.2 Hz, 1H), 7.37–7.62 (m, 5H), 7.73 (s, 1H), 8.05 (d, J = 7.9 Hz, 1H), 8.12 (d, J = 7.7 Hz, 1H), 11.24 (s, 1H); 13.62 (s, 1H) ppm; ^{13}C NMR (DMSO-d_6, 100 MHz) δ: 18.74, 56.38, 75.75, 110.78, 111.63, 116.82, 120.16, 121.09, 121.56, 122.69, 123.08, 123.15, 125.80, 127.09, 128.12, 132.52, 134.86, 139.29, 143.17, 148.97, 150.80, 153.97, 162.90, 167.38, 169.16 ppm; Anal. Calcd for $C_{25}H_{20}N_4O_4S$: C, 63.55; H, 4.27; N, 11.86. Found: C, 63.56; H, 4.26; N, 11.87.

*4.1.1.5.18. 2-(4-(Benzo[d]thiazol-2-yl)-2-methoxyphenoxy)-N′-(5-nitro-2-oxoindolin-3-ylidene) propane hydrazide (**8b**).* Yellow powder; Yield 73%; m.p. 192–195 °C; IR (KBr, cm^{-1}): 3435, 2921, 1706, 1626, 1509, 1482, 1340; ^{1}H NMR (DMSO-d_6, 400 MHz) δ: 1.62 (d, J = 8.0 Hz, 3H), 3.97 (s, 3H), 5.24 (q, 6.5 Hz, 1H), 7.12 (d, J = 8.4 Hz, 1H), 7.25–7.59 (m, 4H), 7.73 (s, 1H), 8.04 (d, J = 7.7 Hz, 1H), 8.11 (d, J = 7.7 Hz, 1H), 8.24–8.29 (m, 2H), 11.88 (br s, 1H), 13.47 (s, 1H) ppm; MS m/z (%): M^+: 517.39 (4.5%), $(M+H)^+$: 518.33 (1.1%); Anal. Calcd for $C_{25}H_{19}N_5O_6S$: C, 58.02; H, 3.70; N, 13.53. Found: C, 58.01; H, 3.72; N, 13.55.

4.2. Biological evaluation

4.2.1. **Antimicrobial activity** [39,40]

4.2.1.1. Test microorganisms. Microbial test strains included *Staphylococcus aureus* (ATCC-29213 and ATCC-6538), *Enterococcus faecalis* (ATCC-29212), *Escherichia coli* (ATCC-25923), *Proteus mirabilis* (ATCC 9240), *Pseudomonas aeruginosa* (ATCC-27953), *Klebsiella pneumoniae* (ATCC-10031 and ATCC-13883), *Shigella flexneri* (ATCC12022) and *Candida albicans* (ATCC-10231).

4.2.1.2. Preparation of microbial inoculums. Microbial inoculums were prepared by subculturing microorganisms into Nutrient Broth (NB) at 37 °C for 18 h. A suspension of the microorganisms was prepared for 18–24 h cultures in NB. A volume of 100 µL of this suspension (10^6 CFU for all bacterial strains and 10^4 CFU for *C. albicans*) was plated on nutrient agar and incubated at 35 °C for 24 h. The addition of the required amount of sterile distilled water was done with the aid of a spectrophotometer at 625 nm (UV Spectrophotometer, Lambda 16, Perkin-Elmer, Langen).

4.2.1.3. Agar diffusion assay. A volume of 100 µL of 2000 µg/mL of all synthesized compounds (**4**, **5**, **6a-j**, **7a-i** and **8a**,**b**) were dissolved in DMSO for the assay of the antimicrobial activity against each of test strains. The plates containing test strains were prepared as mentioned before and the wells were cut using a sterile cork borer of 6 mm diameter. DMSO was used as a negative control. The results were recorded after incubation at 37 °C for 24 h as zone of inhibition in mm.

4.2.1.4. Determination of the minimum inhibitory concentration. The MIC values were determined for the tested compounds (**4**, **5**, **6a-j**, **7a-i** and **8a**,**b**), where two-fold dilution series based on 1000, 500, 250, 125, 62.5, 31.25, 15.62, 7.8, 3.9, 1.95, 0.97, 0.488, 0.244 and 0.122 µg/mL were used for each compound. Ciprofloxacin was used as a standard antibiotic and fluconazole as a standard antifungal drug. Each microorganism was cultured at a cell density 10^6 CFU/mL for all bacterial strains and 10^4 CFU/mL for *C. albicans* and incubated for 24 h at 36 °C ± 1 °C, under aerobic conditions. After incubation, confluent bacterial growth was observed. Inhibition of the bacterial and fungal growth was measured in mm. The MIC values were measured at the concentration of tested compound which did not allow visible growth of the organism.

4.2.2. ***E. coli* DNA gyrase supercoiling assay** [41,42]

Compounds (**4**, **5**, **6c**, **6d**, **6g**, **6i**, **6j**, **7b**, **7c**, **7g** and **8a**) were selected to be tested for their inhibitory activity against *E. coli* DNA gyrase. The assay was performed based on established protocols obtained from the supplier, TopoGEN, Inc. using *E. coli* DNA Gyrase assay kit (TG2000G-1). All of the reactions were stopped by the addition of 10 ml of 3X gel-loading buffer (final concentration: 1.2% SDS, 6 mM EDTA, 10% glycerol, 0.02% bromophenol blue). Twenty ml of this was loaded on a 1% agarose, TAE (40 mM Tris-acetate, 0.01 M EDTA pH 8.3) gel and run for 3–4 h at 60 V. The gel was stained with 0.5 mg/L ethidium bromide in TAE for 30 min while rocking, then destained for 20 min in deionized water. Fluorescent images were captured on a UV transilluminator imaging system at a wavelength of 300 nm. The fluorescence intensity of the supercoiled plasmid reaction product of gyrase was quantitated. The tested compounds were dissolved in DMSO and the assay was performed at concentrations of the selected tested compounds 0.1, 1, 10 and 100 µg/mL. IC_{50} values (µM) were calculated using GraphPad Prism software. Ciprofloxacin was used as a positive control. The experiments were done in triplicates.

4.3. Quantitative structure–activity relationship (QSAR) study [31–36]

4.3.1. Drawing structures and molecular descriptors calculation

Compounds'3D structures were built using Molecular Operating Environment (MOE, 2010.10) software, the built compounds were then energy minimized. All structure minimizations were performed with MOE until an RMSD gradient of 0.05 $kcal{\cdot}mol^{-1}$ $Å^{-1}$ with MMFF94x force field and the partial charges were automatically calculated. Finally, a set of 313 molecular mechanical descriptors was calculated

for all compounds using MOE.

4.3.2. Training set and test set generation

The 15 newly synthesized benzothiazole derivatives were divided into a training set of 12 compounds and an external validation test set of 3 compounds. Training and test sets were then saved as "comma delimited" files (.csv).

4.3.3. QSAR model generation and validation

4.3.3.1. Target property manipulation. For model generation, the anti-microbial activity which is expressed as MIC (μM) was converted to (1/MIC) for mathematical convenience and to have the parameter representing the activity directly proportional to the potency, i.e. the higher the 1/MIC value for a compound the higher its anti-microbial activity, what facilitates the model generation.

4.3.3.2. Descriptor filtration. It is worth mentioning that model generation was carried out using the training set only, whereas the test set was kept aside for the validation step. RapidMiner 7.1.000 Basic Edition [31–33] was first used to remove the descriptors which show low variance among the different compounds using "*Remove Useless Attributes*" operator. The descriptors survived this initial filtration step were processed further to construct the QSAR model.

4.3.3.3. Descriptor selection and model generation. Forward selection algorithm (FSA) implemented in RapidMiner 7.1.000 Basic Edition was used to select the descriptors that are most correlated to the anti-microbial activity. Multiple Linear Regression (MLR) implemented in RapidMiner was used as the machine learning algorithm for linear model generation which routinely removes co-linear descriptors. In FSA, Leave-10%-out (L10%O) cross-validation root mean square error ($RMSE_{CV}$) was used to evaluate model performance to select the best model during the descriptor selection step.

4.3.3.4. Model validation. For model validation, L10%O cross-validation was used for model internal validation. Moreover, external validation was performed by using the obtained model for the prediction of the antimicrobial activity of the unseen test set to evaluate the model predictive ability in case of unknown data points which is the real measure of the model reliability and robustness.

4.4. Molecular docking study

All studies of molecular docking were performed using the software Molecular Operating Environment (MOE, 2010.10). All minimizations were performed with MOE until an RMSD gradient of 0.05 kcal·mol^{-1} Å^{-1} with MMFF94x force field and the partial charges were automatically calculated. The X-ray crystallographic structure of *E. coli* DNA gyrase B co-crystallized with a thiazole inhibitor (PDB ID: 4DUH) [37] were retrieved from the protein data bank (PDB), [https://www.rcsb.org/]. Chain B was first removed followed by the removal of water molecules and ligand not involved in binding in the active site. Then, the enzyme structure was prepared for molecular docking using *Protonate 3D* protocol in MOE with the default options. The co-crystalized inhibitor was used to define the active site for molecular docking. Triangle Matcher placement method and London dG scoring function were used in the docking protocol. Docking setup was first validated by self-docking of the co-crystallized inhibitor in the enzyme active site giving a docking pose with an energy score (S) = −14.46 kcal/mol and an RMSD of 0.432 Å from the co-crystalized ligand pose (Figs. 6 and 7). The validated molecular docking setup was then used to investigate the ligand-target interactions of the newly synthesized compounds in the *E. coli* DNA gyrase B active site to predict their binding pattern and to investigate their ability to satisfy the required structural features for binding interactions (Figs. 8 and 9) (for further details see Supplementary information).

Acknowledgments

The authors thank the National Research Centre (NRC) - Cairo - Egypt for the financial support (2018-2019) of this manuscript through the project No. AR110218.

Appendix A. Supplementary material

Supplementary data to this article can be found online at https://doi.org/10.1016/j.bioorg.2019.103373.

References

[1] M. Durcik, D. Lovison, Z. Skok, C.D. Cruz, P. Tammela, T. Tomasic, D.B. Tiz, G. Draskovits, A. Nyerges, C. Pal, J. Ilas, L.P. Masic, D. Kikelj, N. Zidar, New N-phenylpyrrolamide DNA gyrase B inhibitors: optimization of efficacy and antibacterial activity, Eur. J. Med. Chem. 154 (2018) 117–132.
[2] I.A. Yule, L.G. Czaplewski, S. Pommier, D.T. Davies, S.K. Narramore, C.W. Fishwick, Pyridine-3-carboxamide-6-yl-ureas as novel inhibitors of bacterial DNA gyrase: structure based design, synthesis, SAR and antimicrobial activity, Eur. J. Med. Chem. 86 (2014) 31–38.
[3] R. Leclercq, Epidemiological and resistance issues in multidrug-resistant staphylococci and enterococci, Clin. Microbiol. Infect. 15 (2009) 224–231.
[4] M. Gjorgjieva, T. Tomašič, M. Barančokova, S. Katsamakas, J. Ilaš, P. Tammela, L.P. Mašič, D. Kikelj, Discovery of benzothiazole scaffold-based DNA gyrase B inhibitors, J. Med. Chem. 59 (2016) 8941–8954.
[5] L.C. Axford, P.K. Agarwal, K.H. Anderson, L.N. Andrau, J. Atherall, S. Barker, J.M. Bennett, M. Blair, I. Collins, L.G. Czaplewski, D.T. Davies, C.T. Gannon, D. Kumar, P. Lancett, A. Logan, C.J. Lunniss, D.R. Mitchell, D.A. Offermann, J.T. Palmer, N. Palmer, G.R. Pitt, S. Pommier, D. Price, B.N. Rao, R. Saxena, T. Shukla, A.K. Singh, M. Singh, A. Srivastava, C. Steele, N.R. Stokes, H.B. Thomaides-Brears, E.M. Tyndall, D. Watson, D.J. Haydon, Design, synthesis and biological evaluation of alpha-substituted isonipecotic acid benzothiazole analogues as potent bacterial type II topoisomerase inhibitors, Bioorg. Med. Chem. Lett. 23 (2013) 6598–6603.
[6] M. Barančoková, D. Kikelj, J. Illaš, Recent progress in the discovery and development of DNA gyrase B inhibitors, Future Med. Chem. 10 (2018) 1207–1227.
[7] D.E. Ehmann, S.D. Lahiri, Novel compounds targeting bacterial DNA topoisomerase/DNA gyrase, Curr. Opin. Pharmacol. 18 (2014) 76–83.
[8] A. Maxwell, DNA gyrase as a drug target, Trends Microbol. 5 (1997) 102–109.
[9] T. Khan, K. Sankhe, V. Suvarna, A. Sherje, K. Patel, B. Dravyakar, DNA gyrase inhibitors: progress and synthesis of potent compounds as antibacterial agents, Biomed. Pharmacother. 103 (2018) 923–938.
[10] S.L. Badshah, A. Ullah, New developments in non-quinolone-based antibiotics for the inhibiton of bacterial gyrase and topoisomerase IV, Eur. J. Med. Chem. 152 (2018) 393–400.
[11] T. Tomasic, L. Masic, Prospects for developing new antibacterials targeting bacterial Type IIA topoisomerases, Curr. Topics Med. Chem. 14 (2014) 131–151.
[12] Z. Jakopin, J. Ilas, M. Barancokova, M. Brvar, P. Tammela, M.S. Dolenc, T. Tomasic, D. Kikelj, Discovery of substituted oxadiazoles as a novel scaffold for DNA gyrase inhibitors, Eur. J. Med. Chem. 130 (2017) 171–184.
[13] P. Dhiman, N. Arora, P.V. Thanikachalam, V. Mogan, Recent advances in the synthetic and medicinal perspective of quinolones: a review, Bioorg. Chem. 92 (2019) 103291.
[14] K. Drlica, X. Zalao, DNA gyrase, topoisomerase IV, and the 4-quinolones, Microbiol. Mol. Biol. Rev. 61 (1997) 377–392.
[15] P.F. Chan, V. Srikannathasan, J. Huang, H. Cui, A.P. Fosberry, M. Gu, M.M. Hann, M. Hibbs, P. Homes, K. Ingraham, J. Pizzollo, C. Shen, A.J. Shillings, C.E. Spitzfaden, R. Tanner, A.J. Theobald, R.A. Stavenger, B.D. Bax, M.N. Gwynn, Structural basis of DNA gyrase inhibition by antibacterial QPT-1, anticancer drug etoposide and moxifloxacin, Nat. Commun. 6 (2015) 1–13.
[16] E.J. Gentry, Antibiotics and Antimicrobial Agents, in: T.L. Lemke, D.A. Williams, V. F. Roche, S.W. Zito (Eds.), Foy's Principle of Medicinal Chemistry, seventh ed., 2013, pp. 1073–1124 (Chapter 33).
[17] N.G. Mohamed, M.M. Sheha, H.Y. Hassan, L.J.M. Abdel-Hafez, F.A. Omar, Synthesis, antimicrobial activity and molecular modeling study of 3-(5-amino-(2*H*)-1,2,4-triazol-3-yl]-naphthyridinones as potential DNA-gyrase inhibitors, Bioorg. Chem. 81 (2018) 599–611.
[18] Priyanka, V. Singh, Ekta, D. Katiyar, Synthesis, antimicrobial, cytotoxic and E. coli DNA gyrase inhibitory activities of coumarinyl amino alcohols, Bioorg. Chem. 71 (2017) 120–127.
[19] P.F. Chan, T. Germe, B.D. Bax, J. Huang, R.K. Thalji, E. Bacqué, A. Checchia, D. Chen, H. Cui, X. Ding, K. Ingraham, L. McCloskey, K. Raha, V. Srikannathasan, A. Maxwell, R.A. Stavenger, Thiophene antibacterials that allosterically stabilize DNA-cleavage complexes with DNA gyrase, PNAS 114 (2017) E4492–E4500.
[20] H. O'Dowd, D.E. Shannon, K.R. Chandupatla, V. Dixit, J.J. Engtrakul, Z. Ye, S.M. Jones, C.F. O'Brien, D.P. Nicolau, P.R. Tessier, J.L. Crandon, B. Song, D. Macikenas, B.L. Hanzelka, A. Le Tiran, Y.L. Bennani, P.S. Charifson, A.L. Grillot, Discovery and characterization of a water-soluble Prodrug of a dual inhibitor of bacterial DNA gyrase and topoisomerase IV, ACS Med. Chem. Lett. 6 (2015) 822–826.
[21] M.A. Azam, J. Thathan, S. Jubie, Dual targeting DNA gyrase B (GyrB) and

topoisomerse IV (ParE) inhibitors: a review, Bioorg. Chem. 62 (2015) 41–63.
[22] T. Tomasic, M. Barancokova, N. Zidar, J. Ilas, P. Tammela, D. Kikelj, Design, synthesis, and biological evaluation of 1-ethyl-3-(thiazol-2-yl)urea derivatives as Escherichia coli DNA gyrase inhibitors, Arch. Pharm. Chem. Life Sci. 351 (2018) e1700333.
[23] M. Durcik, P. Tammela, M. Barancokova, T. Tomasic, J. Ilas, D. Kikelj, N. Zidar, Synthesis and evaluation of N-phenylpyrrolamides as DNA gyrase B inhibitors, ChemMedChem 13 (2018) 186–198.
[24] H.J. Boehm, M. Boehringer, D. Bur, H. Gmuender, W. Huber, W. Klaus, D. Kostrewa, H. Kuehne, T. Luebbers, N. Meunier-Keller, F. Mueller, Novel inhibitors of DNA gyrase: 3D structure based biased needle screening, hit validation by biophysical methods, and 3D guided optimization. a promising alternative to random screening, J. Med. Chem. 43 (2000) 2664–2674.
[25] M. Oblak, M. Kotnik, T. Solmajer, Discovery and development of ATPase inhibitors of DNA gyrase as antibacterial agents, Curr. Med. Chem. 14 (2007) 2033–2047.
[26] M. Singh, S. Sellamuthu, S. Kumar Singh, M. Gangwar, G. Nath, S.K. Singh, Antimicrobial potency and molecular mechanism of benzothiazole Schiff base hybrids, Saudi J. Med Pharm. Sci. 3 (2017) 1360–1369.
[27] M. Singh, S.K. Singh, M. Gangwar, G. Nath, S. Singh, Design, synthesis and mode of action of some benzothiazole derivatives bearing an amide moiety as antibacterial agents, RSC Adv. 4 (2014) 19013–19023.
[28] L.W. Wattenberg, M.A. Page, J.L. Leong, Induction of increased benzpyrene hydroxylase activity by 2-phenylbenzothiazoles and related compounds, Cancer Res. 28 (1968) 2539–2544.
[29] S. Bazile, N. Moreau, D. Bouzard, M. Essiz, Relationships among antibacterial activity, inhibition of DNA gyrase, and intracellular accumulation of 11 fluoroquinolones, Antimicrob. Agents Chemother. 36 (1992) 2622–2627.
[30] J.M. Domagala, Structure-activity and structure-side-effect relationships for the quinolone antibacterials, J. Antimicrob. Chemother. 33 (1994) 685–706.
[31] RapidMiner 7.1.000 Basic Edition; RapidMiner GmbH: Dortmund, Germany, 2016.
[32] I. Mierswa, M. Wurst, R. Klinkenberg, M. Scholz, T. Euler, YALE: rapid prototyping for complex data mining tasks, in: Proceedings of the 12th ACM SIGKDD international conference on Knowledge discovery and data mining, ACM, Philadelphia, PA, USA, 2006.
[33] O. Ritthoff, R. Klinkenberg, S. Fisher, I. Mierswa, S. Felske, YALE: Yet Another Learning Environment., in LLWA'01 - Tagungsband der GI-Workshop-Woche Lernen - Lehren - Wissen Adaptivitat. University of Dortmund, Dortmund, Germany. Technical Report, 2001, pp. 84-92.
[34] S.S. Abd El-Karim, Y.M. Syam, A.M. El Kerdawy, T.M. Abdelghany, New thiazol-hydrazono-coumarin hybrids targeting human cervical cancer cells: Synthesis, CDK2 inhibition, QSAR and molecular docking studies, Bioorg. Chem. 86 (2019) 80–96.
[35] M. Shahlaei, Descriptor selection methods in quantitative structure-activity relationship studies: a review study, Chem. Rev. 113 (2013) 8093–8103.
[36] G. Cruciani, P. Crivori, P.-A. Carrupt, B. Testa, Molecular fields in quantitative structure–permeation relationships: the VolSurf approach, J. Mol. Structure (Theochem) 503 (2000) 17–30.
[37] M. Brvar, A. Perdih, M. Renko, G. Anderluh, D. Turk, T. Solmajer, Structure-based discovery of substituted 4,5'-bithiazoles as novel DNA gyrase inhibitors, J. Med. Chem. 55 (2012) 6413–6426.
[38] Y.M. Ha, J.Y. Park, Y.J. Park, D. Park, Y.J. Choi, J.M. Kim, E.K. Lee, Y.K. Han, J.A. Kim, J.Y. Lee, H.R. Moon, H.Y. Chung, Synthesis and biological activity of hydroxy substituted phenyl-benzo[*d*]thiazole analogues for antityrosinase activity in B16 cells, Bioorg. Med. Chem. Lett. 21 (2011) 2445–2449.
[39] F.C. Tenover, M.V. Lancaster, B.C. Hill, C.D. Steward, S.A. Stocker, G.A. Hancock, C.M. O'Hara, S.K. McAllister, N.C. Clark, K. Hiramatsu, Characterization of staphylococci with reduced susceptibilities to vancomycin and other glycopeptides, J. Clin. Microbiol. 36 (1998) 1020–1027.
[40] A.W. Bauer, W.M. Kirby, J.C. Sherris, M. Turck, Antibiotic susceptibility testing by a standardized single disk method, Am. J. Clin. Pathol. 45 (1996) 493–496.
[41] J.W. Phillips, M.A. Goetz, S.K. Smith, D.L. Zink, J. Polishook, R. Onishi, S. Salowe, J. Wiltsie, J. Allocco, J. Sigmund, K. Dorso, S. Lee, S. Skwish, M. de la Cruz, J. Martín, F. Vicente, O. Genilloud, J. Lu, R.E. Painter, K. Young, K. Overbye, R.G.K. Donald, S.B. Singh, Discovery of Kibdelomycin, a potent new class of bacterial Type II topoisomerase inhibitor by chemical-genetic profiling in Staphylococcus aureus, Chem. Biol. 18 (2011) 955–965.
[42] A. Maxwell, N.P. Burton, N. O'Hagen, High-throughput assays for DNA gyrase and other topoisomerases, Nucl. Acids Res. 34 (2006).